EXPLORATION OF A MINE WASTE DUMP FAILURE

By

Rui Miguel Figueiredo Lopes Pereira

Thesis submitted for the
Degree of Master of Science in Engineering
Chania - June, 2018

Technical University of Crete

School of Mineral Resources Engineering

Title: EXPLORATION OF A MINE WASTE DUMP SITE FAILURE

Author: Rui Miguel Pereira

Email: Lpereira.rui@gmail.com

University: Technical University of Crete

School of Mineral Resources Engineering

Master´s committee:

Ass. Professor Dr. Steiakakis, Emmanouil
School of Mineral Resources Engineering
Technical University of Crete, Greece

Professor Dr. Exadaktylos, George
School of Mineral Resources Engineering
Technical University of Crete, Greece

Professor Dr. Galetakis, Michalis
School of Mineral Resources Engineering
Technical University of Crete, Greece

The views and conclusions contained in this document express the author and should not be taken as necessarily representing the views of the examiners.

AKNOWLEDGEMENTS

ABSTRACT

Nowadays the mining exploration is the aim of several studies in order to exploit in a safe, orderly and sustainable way all mine material of economic or no economic value.

Focusing on the material with no economic value that represents large volumes of waste soil material is going to be deposited in areas properly chosen and close as possible of the open pits where the waste is produced. These volumes after a few stages of deposition give rise to enormous masses of soil material named waste dumps. Due to their gradual depositions and different water conditions that can be present, the study of their stability becomes necessary, in order to avoid hazards that can put at risk operations, equipment and above all human lives.

In this thesis, analysis of a waste dump stability on a Lignite Mine located in northern Greece was carried out using two different soil models in Plaxis 2D.

In the first scenario the kinetic behaviour of all the formations was simulated using the Mohr Coulomb model.

In the second scenario, the clayey layer located in the base of deposition was simulated using Softening Soil Model, while the remaining layers were simulated using the Mohr Coulomb criterion.

Comparing the simulation results with the records in the field, the importance of using the appropriate behavioral criterion for each individual layer in order to achieve the optimum result is highlighted.

Keywords: Soft Soil model, Mohr-Coulomb model, Waste dump, Clayey layer, Plaxis 2D.

Περίληψη

Σήμερα η εκπόνηση μεταλλευτικών μελετών έχει ως στόχο η εκμετάλλευση των ορυκτών πρώτων υλών να γίνεται με ασφάλεια, ορθολογικά και με βιώσιμο τρόπο.

Το στείρο υλικό το οποίο συχνά αποτίθεται εσωτερικά ή εξωτερικά του ορυχείου δημιουργεί τεράστιες μάζες εδαφικού υλικού. Λόγω της σταδιακής αύξησης του ύψους των αποθέσεων, η μελέτη ευστάθειας της μάζας καθίσταται επιτακτική προκειμένου να αποφευχθεί κάθε τυχόν αστοχία που θέτει σε κίνδυνο τις επιχειρήσεις, τον εξοπλισμό και πάνω απ' όλα την ανθρώπινη ζωή.

Σε αυτή τη διατριβή, πραγματοποιήθηκε ανάλυση απόθεσης στείρων υλικών λιγνιτωρυχείου στη Β. Ελλάδα χρησιμοποιώντας δύο διαφορετικά μοντέλα συμπεριφοράς εδάφους και το λογισμικό Plaxis 2D. Σε πρώτη φάση η συμπεριφορά όλων των σχηματισμών προσομοιώθηκε χρησιμοποιώντας το μοντέλο Mohr Coulomb. Σε δεύτερη φάση, το στρώμα της αργίλου το οποίο απετέθη στη βάση της απόθεσης, προσομοιώθηκε με το μοντέλο συμπεριφοράς Softening Soil Model, ενώ τα υπόλοιπα στρώματα της απόθεσης με βάση το κριτήριο Mohr Coulomb.

Η σύγκριση των αποτελεσμάτων προσομοίωσης της κινητικής συμπεριφοράς της απόθεσης με τις καταγραφές στο πεδίο, αναδεικνύει την σπουδαιότητα χρήσης του κατάλληλου μοντέλου συμπεριφοράς των επιμέρους στρωμάτων προκειμένου να επιτευχθεί το βέλτιστο αποτέλεσμα προσομοίωσης.

TABLE OF CONTENTS

LIST OF FIGURES

LIST OF TABLES

CHAPTER 01 Introduction

1.1 BACKGROUND

The present work was performed in the context of an investigation of major failure that occurred in a Mine waste dump in North of Greece.

The instability had a mobilization capacity with an outcome of 40 Mm^3 of mass volume followed by a flow of 2.5 Mm^3 of materials being discharge on outside limits. Initially the failure had a mass of permanent movement ranging from 30 to 90 m, while the distance between the toe and the crown of the blade was 1100 m with a width in the foot of 550 m. Over time, materials that flowed out of the boundaries of the deposit attained a distance of 300 m away from the original foot of dump deposit.

In order to stabilize the failure, inhibitory dams were made. The first attempt was constructed on 2004 reaching 20 m high, but it was discarded before its completion, because the sliding mass reached the dam. Nonetheless, the constructed barrier had a retarding effect on the sliding mass by slowing the movement rate.

On the second (and last) stabilization dam a distance of about 300 m from the original toe of the dump slope was implemented. At the end of construction the dam presented a final length of 1500 m has a variable trapezoidal cross-section with a maximum height of 46 m, a width at the top of 40 m, and a maximum width at the base of 200 m [Steiakakis et al., 2009].
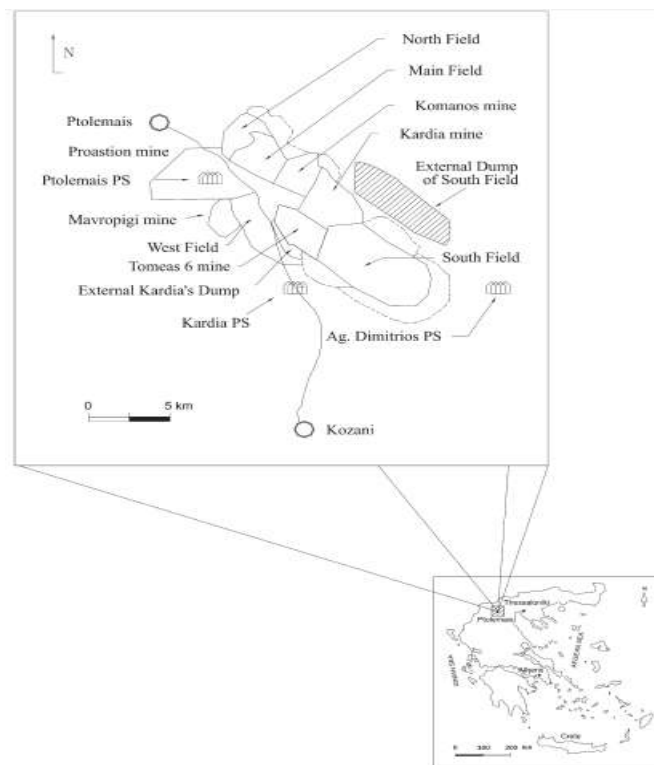
Figure 1: Western Macedonia Lignite Centre [Steiakakis et al., 2009].

1.2 OBJECTIVES

The aim of this thesis is to simulate the deposition process of a waste dump and to investigate the mechanism of failure using the finite element method. The simulation was carried out through the Plaxis 2D by using Soft Soil model as well as the classic Mohr-Coulomb model in order to assess advantages and disadvantages of both models.

1.3 STRUCTURE OF THE DISSERTATION

The development of this thesis occurs as follows:

- Chapter 1: Begins with an overall presentation of the thesis, as well as an approach to the ambitions and problems addressed in the course of this work.
- Chapter 2: Presents a literature review of some topics such as dump failure modes and mechanisms of failure plus factors that may impact the dump stability. The main geotechnical properties of the soil formations were also discussed.
- Chapter 3: On this particular chapter we can find a description of the methods frequently applied for investigating the stability of slopes as well as a brief description of Plaxis software and the models used for simulating soil behaviour like Mohr-Coulomb and Soft soil model.
- Chapter 4: Presents a general description of the external dump deposition in which the academic investigation was based.
- Chapter 5: The fifth chapter deals with a computer simulation process using the finite element method. Description of the models, steps used, geotechnical parameters of soil materials considered, as well as the results of the solutions are presented.
- Chapter 6: Finally, sixth chapter presents the main conclusions of the process simulation and respective recommendations as well.

CHAPTER 02 Literature review

2.1 INTRODUCTION

The mining industry has changed dramatically in the past decades as a consequence of the market demand pushed by new economic powers. This has resulted in new challenges, in terms of technology, production optimization, operations costs, personnel, safety and waste dump management.

In these new challenges one of the most interesting is definitely the waste dumps. Since these types of soil structures in the world today are a major concern and are taken very seriously when designing open mine operations because of the dimensions (height, width and volume) they can assume and the risk they can pose to modern society.

In order to avoid and be ready for these types of threats (e.g. slope failures), useful data of waste soil/rock material properties, as well as foundation conditions should be acquired. Understanding of groundwater along with seepage is essential on design and planning a waste dump; mitigation plans should be delineated as well. This expertise may be acquired from field studies which include geological and geotechnical mapping, sampling, on-site monitoring wells, excavation test pits, sampling waste rock, and foundation materials All these issues impacting dump stability must be evaluated during the project life span of a waste dump [Robertson, 1985].

2.2 DUMP FAILURE MODES AND FAILURE MECHANISM

The different failure modes that take place in mine waste dumps have been summarized by Caldwell and Moss (1984) who review the methods of analysis. Most of these failure modes are shown in Figure 2.

Surface or edge slides may likely take place while the material progresses down the slope. This mode of failure is most expected to appear in end-dumped embankments and is most successfully determined through the equations outlining the stability concerning an infinite slope. When enough water makes its way into in the slope and flows parallel to the face, a shallow flow slide may take place. Dumps placed on flat ground of competent soil are least expected to fail. Even though, if the flat ground is covered by a slim layer of weakened material, base failure may well take place. In case the ground shows some inclination, base failure is most expected to occur. Block displacement is possible to manifest where a dump is actually conceived on inclined ground and the soil cover is fairly thin and sensitive. Abnormally high water tables in the embankment, earthquakes or the decay of organic material under the dump may trigger such failure [Robertson, 1985].

a) Surface or edge slide   b) Shallow flow slides

c) Base failure (Spreading)   d) Block translational

e) Circular Arc Failure   f) Foundation circular failure
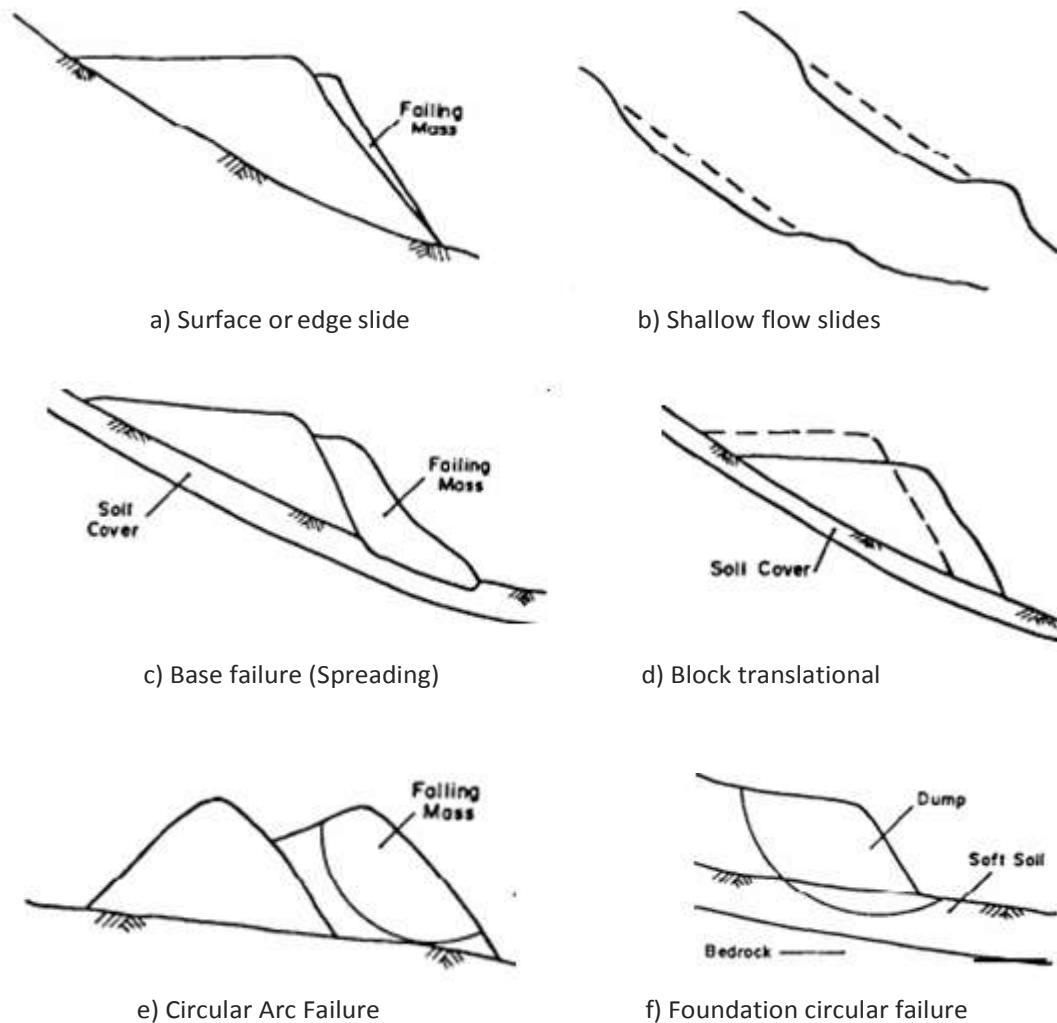
Figure 2: Mine Waste Dumps - possible failure modes [Caldwell et al., 1981].

The failure modes tend to be linked to a mechanism which has been broadly analyzed. Circular arc failure through the dump material is forecast to take place where the dump is created on a competent foundation, and dump material possesses a significant amount of fine grain soil. Similar, a circular arc failure surface could possibly progress throughout a deep foundation soil deposit of fine-grained soils [Robertson, 1985].

2.3 FACTORS AFFECTING DUMP STABILITY

The dimensions and difficulty of the project, in addition to the continuation of dump failure, will decide and manage the extension of the analysis performed in order to acquire the data and parameters needed. The report should be accurate enough to locate all adverse conditions as well as to present reasonable certainty in which the parameters applied in the construction are proper [Orman et al., 2011].

2.3.1 SITE TOPOGRAPHY

Topography data compiled over research phase of design must address the whole drainage area that may possibly jeopardize the dump, and also determining those areas that will be involved in case dump failures actually manifest. In case of failure event, the inclination of the dump foundation will certainly be an essential factor in the dump stability along with run out distance. Practice indicates that foundation slopes higher than 25° usually result in smaller factors of safety concerning slope stability. However, topographical features creating lateral support or toe buttressing will certainly enhance the waste dump stability [Orman et al., 2011].

2.3.2 DUMP GEOMETRY AND STACKING METHOD

The waste dump geometry relies mainly on the dumping method along with the topography at location. The two typical construction techniques for waste dumps consist of end dumping (Fig. 2.1) and stacking material or layers (Fig. 2.2). When the material is end-dumped from the crest of the waste dump, the material are going to run down the slope and rest at or nearby the angle of repose, with the heavier particles rolling down to the toe of the dump [Orman et al., 2011].

When compare, layered or stacked dumps grant a high factor of safety to be kept, due to the fact they are constructed in a more controlled manner starting from the bottom. The layers could certainly be placed and compacted in order to enhance the density as well as the strength of the material. Nevertheless, layered waste dumps are not always recommended, considering they need relatively flat topography [Orman et al., 2011].

Waste dumps built from end dumping method (Fig. 2.1) are most likely to have a loose, collapsible particle structure within the dump as compared with those constructed from the layered method (Fig. 2.2). Collapse will happen in localized arching, which in turn leads to lessen normal pressures and shear strengths [Orman et al., 2011].

Figure 2.1: Dumping method [goodfreephotos.com].

Figure 2.2: Stacking method - Stacker in operation [Steiakakis et al., 2009].

2.3.3 GEOTECHNICAL AND MECHANICAL PROPERTIES OF MINE WASTE

The geotechnical properties of mine waste materials differ considerably regarding projects as well as different stages involving the exact same project. The density, saturation, and also shear-strength parameters of the materials forming the dump influence the slope stability and the estimated factor of safety (FS). Some other useful insight for design involves the particle size distribution, specific gravity, permeability, compression index, and also degradation behaviour of the waste materials. Most of these parameters are typically based on lab tests. Although, field practices and construction procedures are often not totally simulated in the laboratory for a variety of reasons (e.g., equipment limitations, duration and finances restraints), and for that reason professional experience is needed in deciding properties for stability analyses. Verification testing is usually required during construction to guarantee that the parameters applied during the design were realistic, precise, and recommended [Orman et al., 2011].

Being familiar with the shear-strength behaviour of the dump material is essential for examining the slope stability of the waste dump. Waste density and gradation variability, combined with differences in normal and confining stresses (e.g., within the pile versus at the toe or on the slope face), lead in heterogeneous shear strength throughout the pile. Usually, a linear-strength envelope with a single friction-angle value over the entire range of stresses could be assumed for the stability analysis. However, the dump heights achieved these days result in a far broader range of normal stresses in the pile, in which the strength envelope does not always remain linear, and this nonlinearity of the strength envelope should be assumed in the stability analysis [Orman et al., 2011].

Another consideration to take into account during design is the effects of weathering on geotechnical properties. Waste materials that had been assumed durable may

weather or be modified in some other way, which reduces slope stability. At instance, weathering of feldspar-rich rock may possibly result in clay formation, lowering the effective friction angle and inhibiting prompt drainage [Orman et al., 2011].

2.3.4 GEOTECHNICAL PROPERTIES OF FOUNDATION

The geotechnical properties of foundation are a critical factor in the overall stability of the waste dump. The dump-site investigations need to determine the prevalent geology of the site as well as any geologic adversity and soil conditions. The soil cover and rock weathering depths needs to be estimated and the materials must be characterized for design. Particular attention must be given to the existence of shallow groundwater, landslides, creeping slopes, organic soils, clays, and also dip slope bedrock structures [Orman et al., 2011].

The subsurface investigation might consist of sampling, in-situ testing, and borehole geophysics, in order to attaining the most important parameters for site design. Subsequently soil and rock samples that have been collected during the investigation, laboratory assessment should be carried out to determine the relevant geotechnical properties of the materials. The classification, strength, permeability, and consolidation properties of the foundation materials, and exactly how these properties can be affected by time or saturation, should be examine. The shear strength and thickness of the foundation soil is definitely a significant parameter for slope stability and the dump failure mode. Permeability of the material at the foundation will most likely impact the generation of pore water pressures in the foundation, impacting the dump stability and reducing the permissible dumping rate [Orman et al., 2011].

Foundations that consist of low-plasticity silts and also clay soils have become responsible for developing shear failure surfaces of countless large dump failures. Consolidation parameters are utilized to computing expected settlement of the foundation [Orman et al., 2011].

2.3.5 GROUNDWATER AND PHREATIC SURFACE

The impact of water when it comes to stability of mine waste dumps might be challenging to assess, and precautions must be considered to avoid excess of water from getting into the dump. As part of assess stability of the waste dump, a seepage assessment must be conducted to determine flows along the dump as well as the height of the phreatic surface. Water pressure accumulate inside of the dump is going to reduce the FS for slope stability, and the potential increment in the phreatic surface need to be considered. An increment in the foundation water table should also be considered since it can lessen the FS with regard to a deep failure by the foundation material, whereas perched water within the dump may result to surface failures. Flow parallel to the surface of the slope is likely to reduce the FS greatly [Orman et al., 2011].

For waste dumps, the biggest stability threat posed by earthquakes is usually liquefaction of foundation materials, despite the fact that liquefaction might happen in susceptible waste materials as well. In case liquefaction happens in the foundation, the whole dump may possibly be translated or there might be progressive failure. Liquefaction as a result of seismic events is generally limited to 20 m in-depth or shallower, as a result of the advantageous effects of confining pressure against liquefaction susceptibility [Orman et al., 2011].

2.3.6 SEISMIC FORCES

At seismically active areas, the slope stability of the waste structure needs also to be analyzed concerning seismic load conditions. The seismic loading, despite the fact of being dynamic and cyclic in nature, is commonly addressed as a superimposed equivalent set of static loads, and the stability analysis for these circumstances is known as the pseudostatic analysis. On these types of analyses, the two-dimensional mass in the limit equilibrium slope-stability model is presented to a horizontal acceleration, which represents inertia forces as a result to earthquake shaking and is equal to an earthquake coefficient multiplied by acceleration of gravity.

The earthquake coefficient, or pseudostatic coefficient, is chosen depending on a specified design earthquake. Usually a percentage of the maximum design acceleration in bedrock can also be used for the pseudostatic analysis. However, selection of a proper pseudostatic coefficient may be dependent heavily on engineering sagacity and can be frequently arguable.

Furthermore, materials within the waste dump may experience a considerable reduction of strength during earthquake shaking that may possibly not be totally comprehended or determined from the research laboratory investigation. For that reason, while pseudostatic analyses are a simplified and convenient tool, they should serve primarily as a screening method as to whether significant displacement may take place during the design earthquake.

If a minimal FS is computed at the pseudostatic analysis (e.g., <1.0), subsequently considerable displacements may well manifest, and displacement (deformation) analyses must be carried out. Dynamic analyses using numerical tools offer an even more sophisticated alternative to pseudostatic analyses. Analyses can be conducted with tools such as the finite difference software, and available finite element method and boundary element method programs. Application of these tools during the design may rely on project spending plan, design requirements, as well as available resources [Orman et al., 2011].

CHAPTER 03 Methods of Slope Stability Analysis

3.1 METHODS FOR INVESTIGATION OF STABILITY OF SLOPES

The stability of dump slope is dictated on the basis of material properties, geometry, foundation conditions, hydraulic factors, and external forces. Effective evaluation of foundation conditions and material properties are essential to acquire knowledge of potential dump behavior. The failure modes that are defined as critical to dump stability need to be subjected to detail study. Proper dump stability monitoring programs are chosen based on evaluation of results, practical mining considerations, effects of instability, and other associated factors [Chaulya et al., 2016].

Different methods for assessing the different modes of failure are briefly explained at next and described in Table 1, along with a discussion of their strengths and restrictions.

3.2 SLOPE STABILITY CHARTS METHOD

Stability charts and tables offer a fast and economical method for evaluating embankment stability. For small, simple and low hazard dumps, stability chart solutions may possibly be all that is needed for the design. They are also useful for exploratory assessments of stability, or to confirm the credibility of outcomes from more advanced analyses.

It is worthwhile to mention that stability charts provide estimated solutions only, and are unable to model advanced failure modes. Therefore, whenever precision is crucial, such as for large or possibly potentially hazardous dumps, or even where advanced failure modes manifest, stability charts are not advised as the only research method. [British Columbia Mine Dump Committee, 1991].

3.3 LIMIT EQUILIBRIUM METHODS

Limit equilibrium methods are normally the most widely selected solutions in slope stability analysis. The essential principle in these methods is in fact that failure will take place through sliding of a mass along a slip surface. The notoriety of the limit equilibrium methods is mostly because of their relative simplicity, the ability to examine the sensitivity of stability to various input parameters, aligned with the geotechnical experience that engineer acquired during several years in estimating the factor of safety [Hamdhan, 2013].

The assumptions in the limit equilibrium methods happen to be that the failing soil mass might be split into slices and that forces act between the slices while different

assumptions are made with regard to these forces in different methods. A few common features and limitation for equilibrium methods in slope stability analysis are described in Table 1. All the methods utilize the same definition concerning the factor of safety:

$$FS = \frac{Shear\ strength\ of\ soil}{Shear\ stress\ required\ for\ equilibrium}$$

The factor of safety is the factor by which the shear strength of the soil would have to be divided to carry the slope into a state of barely stable equilibrium [Hamdhan, 2013].

The outcomes linked to the accuracy of the limit equilibrium methods can be reviewed as follows:

1) Concerning effective stress analysis of slopes, the ordinary method of slices (OMS) is clearly inaccurate. The computed factor of safety is actually too low. This method is relatively precise for any type of total stress analysis using circular slip surfaces. The method does not have numerical problems.

2) For most conditions, the Bishop's modified method is reasonably accurate (apart from when numerical problems are found). Its limitations are that it is suitable just for circular slip surfaces, and that it has numerical problems under some conditions. If a factor of safety is determined using Bishop's modified method that is lower than the factor of safety concerning the same circle calculated using the ordinary method of slices (OMS), it can be deduced that there are numerical problems with the Bishop's modified method analysis. The OMS factor of safety is a preferable solution in such situations. For this reason it is a good strategy to estimate the OMS value regarding the factor of safety (FS) for every single circle whenever the Bishop's modified method is applied, in order to compare both values.

3) The calculated factor of safety through force equilibrium methods gets sensitive to the assumption of the inclination of side forces between slices. A poor assumption regarding side force inclination will alter the reliability of the factor of safety.

4) Janbu's, Morgenstern and Prices's and Spencer's method which meet all the conditions of equilibrium tend to be accurate for any conditions. All of these methods encounter numerical problems under some circumstances [Duncan, 1996].

Table 1 - Features & Limitation for the Equilibrium Methods in Slope Stability Analysis [Duncan, 1996].

Method	Features and Limitations
Slope Stability Charts (Janbu, 1968, Duncan et al, 1987)	▪ Accurate enough for many applications. ▪ Faster when compared with detailed computer assessment.
Ordinary Method of Slices (Fellenius, 1927)	▪ Only applies to circular slip surfaces. ▪ Satisfies moment equilibrium. ▪ Fail to satisfy horizontal or vertical force equilibrium.
Bishop's Modified Method (Bishop, 1955)	▪ Only for circular slip surfaces. ▪ Satisfies moment equilibrium. ▪ Meet vertical force equilibrium. ▪ Does not meet horizontal force equilibrium.
Force Equilibrium Methods (e.g. Lowe and Karafiath, 1960, Army Corps of Engineers, 1970)	▪ Covers any form of slip surfaces. ▪ Does not meet moment equilibrium. ▪ Meet both vertical and horizontal force equilibrium.
Janbu's Generalized Procedure of Slices (Janbu, 1968)	▪ Covers any shape of slip surfaces. ▪ Meet all conditions of equilibrium. ▪ Allow side force locations to be varied. ▪ More frequent numerical problems than some other methods.
Morgenstern and Price's Method (Morgenstern and Price, 1965)	▪ Any shape of slip surfaces. ▪ Meet all conditions of equilibrium. ▪ Allow side force orientations to be varied.
Spencer's Method (Spencer, 1967)	▪ Covers any shape of slip surfaces. ▪ Meet all conditions of equilibrium. ▪ Side forces are assumed to be parallel.

3.4 FINITE ELEMENT METHOD

The finite element method is a general-purpose method that has many appealing capabilities for analysis of stresses and movements in earth masses.

▪ It has been used to estimate stresses, movements, and also pore pressures in embankments and slopes.
▪ It has been applied for analyses of conditions during the course of construction, as well as after construction, as consolidation or swelling manifest and excess pore pressures dissipate.
▪ It has been used to study the likelihood of cracking, local failure, and overall stability of slopes.

The method is so generic that it is feasible to model many complex conditions with high level of accuracy, including in the analyses such as nonlinear stress-strain behaviour, non homogeneous conditions, as well as changes in geometry throughout construction of an embankment or an excavation [Duncan, 1996].

In the finite element method, one of the techniques that can be applied is shear strength reduction (SSR). In which the angle of dilatancy as well as soil modulus is not really important parameters in this technique. The safety factor can be acquired, presuming a Mohr-Coulomb failure criterion, by lowering the strength parameters gradually, beginning with unfactored values $\varphi_{available}$ and $c_{available}$, until no equilibrium can be found in the calculations. The related strength parameters can be denoted as $\varphi_{failure}$ and $c_{failure}$ and the safety factor η_{fe} is defined as:

$$\eta_{fe} = \frac{\tan \varphi_{available}}{\tan \varphi_{failure}} = \frac{c_{available}}{c_{failure}}$$

There are two possibilities in order to attain the factor of safety as described above.

Method 1: An analysis is conducted with unfactored parameters modelling all construction stages required. The outcomes represent the behaviour for working load conditions at the defined construction steps. This analysis is accompanied by an automatic reduction of strength parameters of the soil until equilibrium can be no longer achieved in the computation. The procedure can be invoked at any construction step. This particular approach is sometimes called as φ/c-reduction technique [Hamdhan, 2013].

Method 2: The analysis is carried out with factored parameters from the outset, i.e. strength values are lowered, again in increments, but a new analysis for all construction stages is conducted for each set of parameters. If sufficiently small increments are used the factor of safety is once again obtained from the computation where equilibrium could not be accomplished [Hamdhan, 2013].

Both techniques tend to be straightforward to employ when using a standard Mohr-Coulomb failure criterion. In the finite element method, failure takes place naturally through the zones within the soil mass in which the shear strength of the soil is not able to withstand the applied shear stress, therefore there is not require making assumption regarding the shape or location of the failure surface [Hamdhan, 2013].

3.4.1 PLAXIS 2D SOFTWARE

Plaxis 2D is an advanced finite element method software designed for studying two dimensional problems of deformation and also stability in geotechnical engineering. The development of the software began in 1987 at Delft University of Technology. The Plaxis 2D software contains three sub programs which include the input program, the

calculation program and the output program. It performs analysis using either an assumption of plane strain or axial-symmetry with 6-noded or 15-noded triangular elements, see Figure 3.
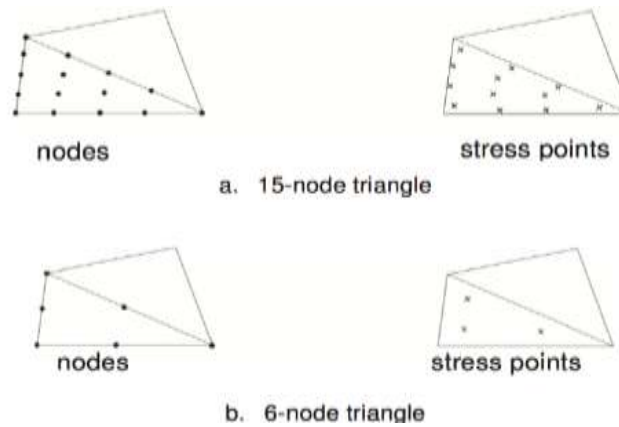
Figure 3: Nodes position and stress points in triangular soil elements [Plaxis, 2012 a].

In case one dimension is substantially larger than the others, it is feasible to utilize the assumption of plane strain. This indicates that the principal strain in the direction of the longest dimension is constrained and assumed to be zero.

To be able to define the deformations of a soil occurring due to variations in the current stress state, a mathematical framework is assigned to the soil. These govern the force displacement interactions and are called material models [Kahlström, 2013].

In Plaxis 2D, there are available a number of material models. However, regarding the aim of this thesis, only the Mohr-Coulomb and Soft Soil material models will be examined.

3.4.2 MODELS FOR SIMULATING SOIL BEHAVIOR
3.4.2.1 MOHR COULOMB MATERIAL MODEL

Understanding of shear strength is needed regarding the resolution of problems involving the stability of soil mass. Whether at a point on any plane within a soil mass the shear stress turns equal to the shear strength of the soil, failure will take place at that point. The shear strength (τ_f) of a soil at a point on a specific plane has been originally explained by Coulomb as a linear function of the normal stress (σ_f) on the plane at the same point [Craig, 1997]:

$$\tau_f = c + \sigma_f \tan\varphi´ \quad \text{Equation 3.1}$$

where C and φ are the shear strength parameters, now defined as cohesion and the angle of shearing resistance, correspondingly. According with Terzaghi's fundamental concept in which shear stress in a soil can be opposed exclusively by the skeleton of

solid particles; shear strength is stated as a function of effective normal stress [Craig, 1997]:

$$\tau_f = c' + \sigma_f' tan\varphi' \quad \text{Equation 3.2}$$

where c' along with φ' are the shear strength parameters in terms of effective stress. Failure will subsequently manifest at any point in which a critical combination of shear stress and also effective normal stress evolves. The shear strength of a soil can also be shown in terms of the effective major and also minor principal stresses (σ_1') and (σ_3') at failure in the point in question. At failure the straight line represented on Eq. 3.2 will be tangential to the Mohr circle symbolizing the state of stress, as displayed in Fig. 3.1, compressive stress being considered as positive. The coordinates involving the tangent point are τ_f and σ_f', where [Craig, 1997]:

$$\tau_f = \frac{1}{2}\left(\sigma_1' - \sigma_3'\right) \sin2\theta \quad \text{Equation 3.3}$$

$$\sigma_f' = \frac{1}{2}\left(\sigma_1' + \sigma_3'\right) + \frac{1}{2}\left(\sigma_1' - \sigma_3'\right) \cos2\theta \quad \text{Equation 3.4}$$
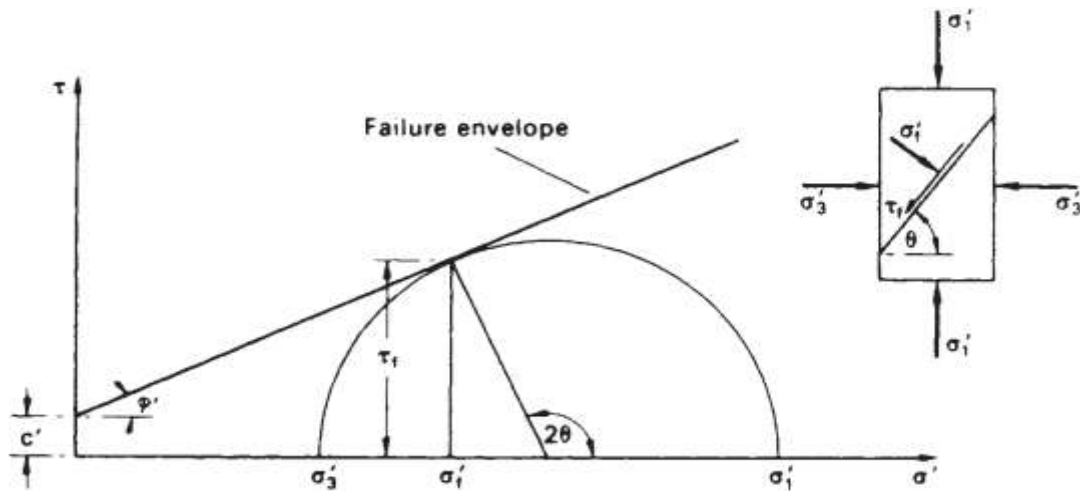
Figure 3.1 Mohr-Coulomb failure criterion and envelope [Craig, 1997].

and θ is the theoretic angle between the major principal plane and the plane of failure. It is noticeable that:

$$\theta = 45° + \frac{\varphi'}{2} \quad \text{Equation 3.5}$$

At Fig. 3.1 the relationship between the effective principal stresses at failure and the shear strength parameters can also be acquired:

$$\sigma_1' = \sigma_3' tan^2\left(45 + \frac{\varphi'}{2}\right) + 2c'\tan\left(45 + \frac{\varphi'}{2}\right) \quad \text{Equation 3.6}$$

Equation 3.6 is known to as the Mohr-Coulomb failure criterion. In case a number of states of stress are identified, each generating shear failure in the soil, the criterion considers that a common tangent, showed by Eq. 3.2, can be drawn to the Mohr circles addressing the states of stress: the common tangent is called the failure envelope of the soil. A state of stress plotting above the failure envelope is not possible. The criterion does not include consideration of strains at, or prior to, failure and indicates that the effective intermediate principal stress has no impact on the shear strength of the soil [Craig, 1997].

The main features of the Mohr-Coulomb material model [Plaxis, 2012b] entail:

- Obeys Hook's Law for isotropic linear elastic behaviour within the yield surface.
- Linear elastic perfectly plastic yield envelope.
- Five input parameters required.

The principal strengths of the Mohr-Coulomb model entail:

- Well-known parameters *E* and *v* used to express stiffness.
- Easy to acquire parameters from separate soil assessments.
- Reliable outcomes for stress states within the elastic region.

The principal weaknesses of the Mohr-Coulomb model entail:

- Constant stiffness with increasing stress in its basic version.
- Unlimited dilatation.
- Does only incorporate ideal-plastic deformations.

3.4.2.2 INPUT PARAMETERS

The soil parameters needed as input for the Mohr-Coulomb model are displayed in Table 2.

Table 2 - Input parameters concerning the Mohr-Coulomb material model [Plaxis, 2012b].

Parameter		Unit
Young´s Modulus	E	KPa
Poisson´s ratio	v	-
Friction angle	ϕ	[˚]
Dilatancy angle	ψ	[˚]
Cohesion	c	KPa

3.4.2.3 SOFT SOIL MODEL

The Soft Soil model considers a logarithmic relation amongst the volumetric strain (ε_v) and the mean effective stress ($p^{'}$) and has strong capabilities when modelling compression behaviour of very soft soils [Plaxis, 2012b]. During isotropic virgin compression, along the normal consolidation line, this relation is formulated as

$$\varepsilon_v - \varepsilon_v^0 = -\lambda^* \ln\left(\frac{p'}{p^0}\right)$$

where λ^* is the modified compression index determining the compressibility of the material during primary loading; p^0 is the initial value of the mean effective stress and ε_v^0 is the initial volumetric strain.

However if the soil is subjected to either unloading or reloading, the behaviour tracks a distinct way and is formulated as

$$\varepsilon_v^e - \varepsilon_v^{e0} = -k^* \ln\left(\frac{p'}{p^0}\right)$$

where k^* is the modified swelling index, ε_v^e is the elastic volumetric strain and ε_v^{e0} is the initial elastic volumetric strain. k^* will establish compressibility regarding the soil material during unloading and subsequent reloading. The distinction amongst the two parameters λ^* and k^* is presented in Figure 3.2.
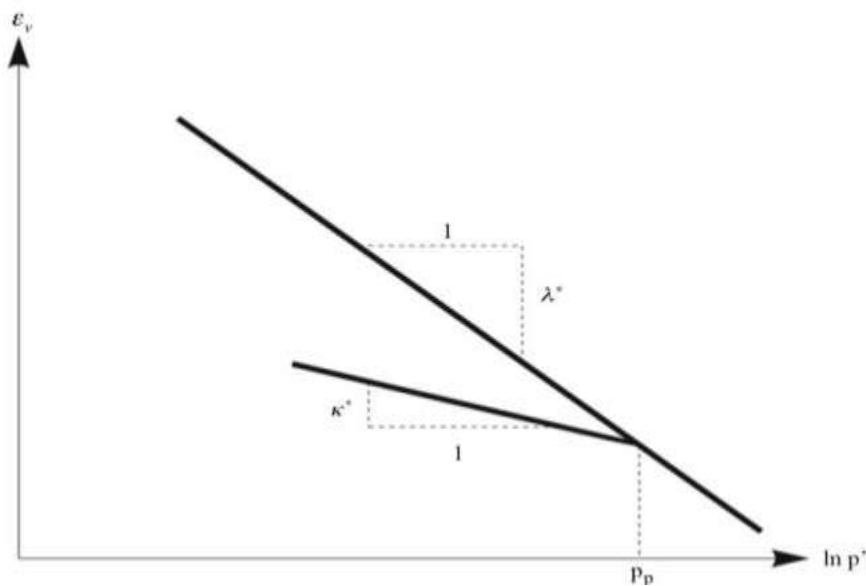
Figure 3.2 Logarithmic relation between volumetric strain and mean effective stress [Plaxis, 2012 b].

An infinite number of unloading and reloading lines might exist in Figure 3.2, each one equivalent to a specific value concerning the isotropic pre-consolidation stress (P_P). The pre-consolidation stress symbolizes the largest stress level experienced by the soil. Throughout unloading and reloading, this pre-consolidation stress stays constant. In primary loading, however, the pre-consolidation stress increases with the stress level, causing irreversible (plastic) volumetric strains [Plaxis, 2012 b].

Differing from Mohr-Coulomb material model, the Soft soil model is capable to account both elastic and plastic material behaviour. It is an advanced constitutive

material model and the principal properties of the Soft Soil model consist of [Plaxis, 2012b]:

- Failure behaviour based on Mohr-Coulomb criterion.
- Yield surface adapt from Modified Cam Clay model with corresponding flow rule for plastic strains.
- Stiffness parameters might be acquired from oedometer-tests.

The principal strengths of the Soft-Soil model entail:

- Stress dependent stiffness (logarithmic compression behaviour).
- Differentiation between primary loading and unloading-reloading.
- Memory for pre-consolidation stress.

The principal weaknesses of the Soft-Soil model entail:

- Not appropriate to other types unless soft soils, normally or near-normally consolidated.
- Secondary compression (creep) is not taken into account.
- Less appropriated for other than compression stress paths.
- Anisotropy of the soil is not taken into consideration.

As can be seen in Figure 3.3, the yield contour assumes an ellipse shape, in which the top intersects with a line having slope M. Where, M represents the critical state line. Nevertheless, in the Soft Soil model, the critical state is not always linked to failure. Alternatively, a Mohr-Coulomb failure criterion is used to get a considerably accurate failure state. Being this criterion a function of the strength parameters (φ and c), that will probably not match to "M Line". The isotropic pre-consolidation stress (PP) establishes the extent of the ellipse along p' axis. Throughout loading, countless ellipses might exist (Fig 3.3) every single referring to a specific value of P_P [Plaxis, 2012 b].
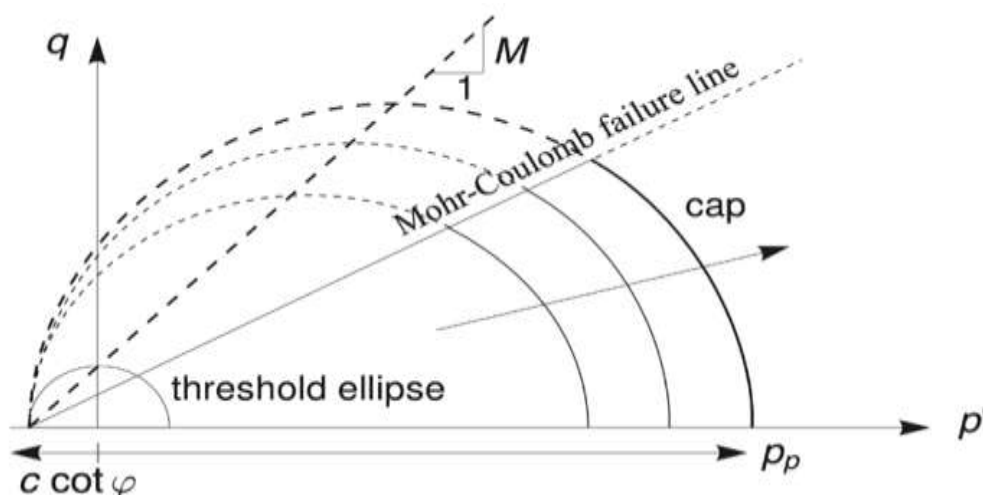

Figure 3.3 Yield surface of the Soft Soil model in p':q-plane [Plaxis, 2012 b].

3.4.2.4 INPUT PARAMETERS

The soil parameters required as input for the Soft Soil model are displayed in Table 3.

Table 3 - Input parameters concerning the Soft Soil material model [Plaxis, 2012 b].

Parameter		Unit
Modified compression index	λ^*	-
Modified swelling index	k^*	-
Friction angle	ϕ	[˚]
Dilatancy angle	ψ	[˚]
Cohesion	c	KPa
Advanced Parameters		Unit
Poisson´s ratio for unloading/reloading	ν_{ur}	-
Coefficient of lateral stress in normal consolidation	K_0^{NC}	-
K_0^{NC} - parameter	M	-

Regarding the Advanced parameters, according with Vermeer when oedometer data is not available when using Soft soil model, a number of empirical relations can been established, relating the modified compression index to different parameters [Vermeer, 2002]. He suggests the following relations in Plaxis 2D:

$$\lambda^* \approx 0{,}3 I_P$$

and

$$\lambda^* \approx 0{,}2(W_L - 0{,}1)$$

Considering the fact that, commonly the ratio ranges between:

$$\frac{\lambda^*}{K^*} \approx 2{,}5 \ to \ 7$$

is possible to compute the modified swelling index K^* [Plaxis, 2018].

CHAPTER 04 General Description of the External dump deposition

4.1 INTRODUCTION

The South Field Mine (SFM) is one of the few active open pit mines, in the Western Macedonia Lignite Centre, which is situated on the north part of Greece in Ptolemais region (110 kilometer west of Thessaloniki). By the end of 2007, the mine was addressing an area around 24 km^2 and operating on ten benches (five for overburden strata plus five for the lignite seams), using mostly the continuous mining method that uses large bucket wheel excavators conveyors and stackers. Furthermore, traditional mining equipment such as heavy trucks, shovels and dozers were utilized for mining the hard rock formations. Activity at the location began on August 1979 and until the end of 2005, 310 Mt of lignite had been generated and 1194 Mm^3 of overburden and inter bedded waste material had been excavated. Until the end of 2007, the rate of extraction was 18–22 Mt of lignite generated per year, by removing a total of more than 100 Mm^3 earth materials.

The soft waste material that was generated from the overburden mining operation was transported by the belt conveys to the adjacent external waste dump, which was positioned NE from the exploitable deposit and designed in three phases addressing a total height of 110 m starting from ground surface. The average inclination of the ground surface along the NE–SW dump axis was around 4%.

At 30 April the year 2004, a significant scale failure began in the middle part of the deposit (Fig. 4), which was tailed by a flow of materials outside the dump limits towards SW. The instability (Figs. 4.1) was characterized by the mobilization of a mass of 40 Mm^3 that was accompanied by a flow 2.5 Mm^3 of materials outside the dump limits. At the initial stage of the failure, the thickness of the moving mass varied around 30 to 90 m, whereas the distance among the toe and the crown of the slide was 1100 m and the width in the foot was about 550 m. With time, the materials that flushed away from the limits of the deposit attained a distance of 300 m from the original foot of the dump deposit [Steiakakis et al., 2009].

The plan for stabilizing the failure required the construction of inhibitory dams. The first was launched in May 2004, presenting a height of 20m, but with no results at the end since the mass reached the site before its completion (Fig. 4.2). Nevertheless, it provided a retarding effect once the sliding mass reached the dam. This obliged the construction of a second stabilization dam planned at a distance of 300 m from the initial toe of the dump slope (Fig. 4). The second dam was characterized by finalized length of 1500 m with variable trapezoidal cross-section, a maximum height of 46 m, and a width of 40 m at the top and 200 m on base. The average slope presented on

second dam was about 25°, the total volume of the material used reaches 2.7 Mm^3, while the expenses of moving the land reached the value of 3.7 M (€). Materials taken from the excavated conglomerate with confirmed quality had been used. Driven by economic sense, over 20% of the dam's building material was original from the sliding mass. This material was properly selected and acquired from sites that would not affect the overall equilibrium [Steiakakis et al., 2009].
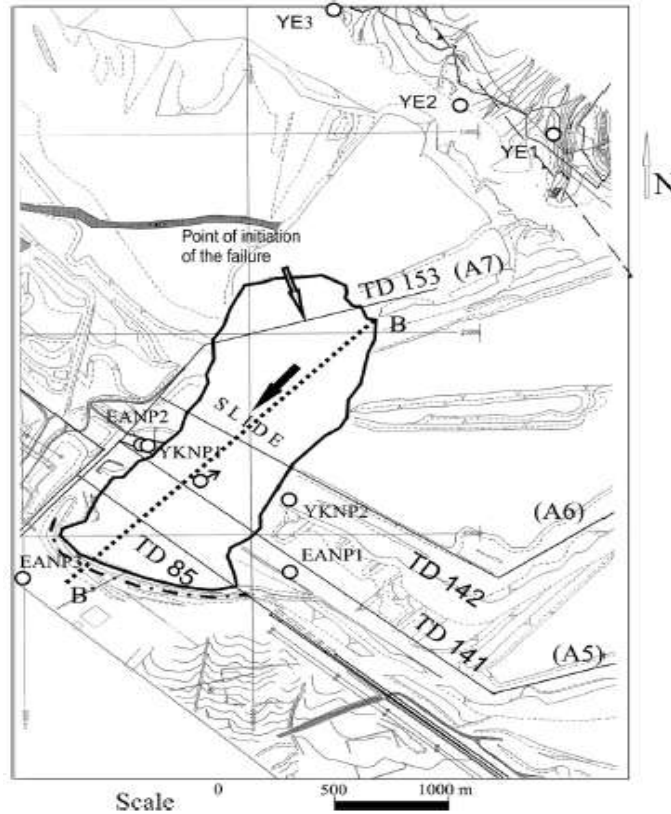

Figure 4.0: Boundaries of the external waste dump failure [Steiakakis et al., 2009].

Figure 4.1: The crest of the dump failure [Steiakakis et al., 2009].

Figure 4.2: The failure moving face plus the first berm under-construction [Steiakakis et al., 2009].

4.2 CONSTRUCTION OF THE EXTERNAL DUMP DEPOSITION

The deposit was design in three stages in an area that includes the "Charavgi's" stream (Fig. 4.3). The ground surface where the dump is located has slope gradient ranging between 2 to 3°, and is prone to slope instability. The first deposition phase involved 30–40 m in thickness of a clay-like material. In the process of stacking, partly overlapped spoil piles of a height 7–8 m were built. Progressively, the stacker was in motion, in order to develop a deposit bench not higher than the aforementioned height. Following, the deposit began again from the starting point of stacking, forming another series of spoil piles [Steiakakis et al., 2009].
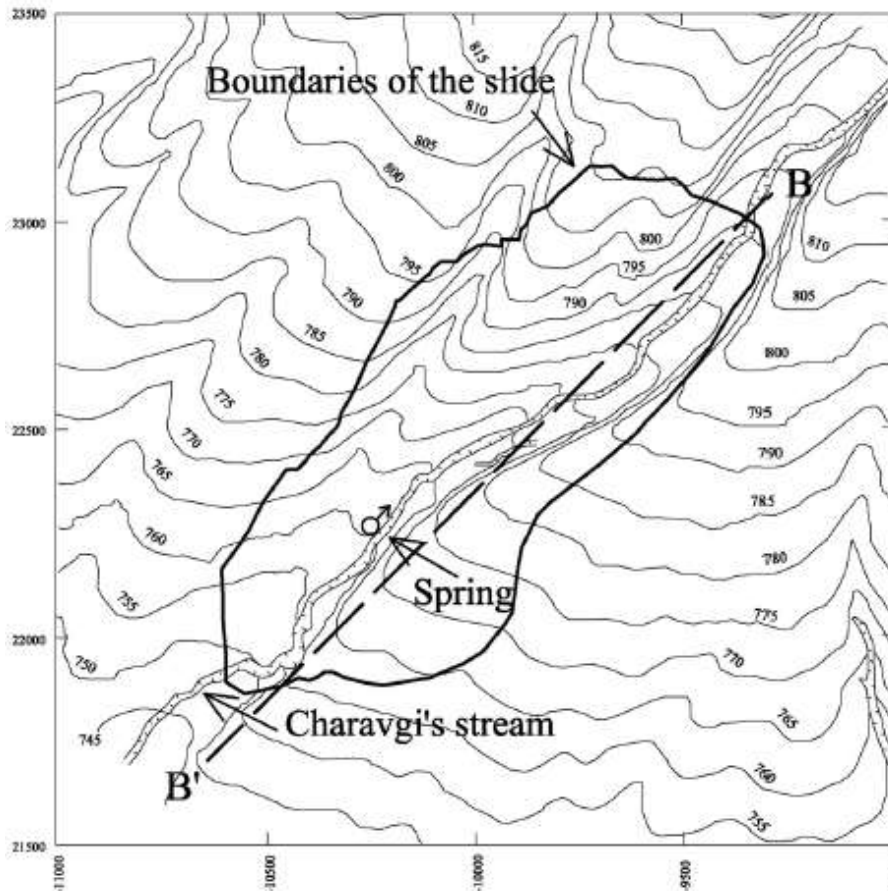

Figure 4.3 The ground surface where the waste dump is located [Steiakakis et al., 2009].

After a set of 4–5 successive runs a dump of a height 30–40 m had been completed. It should be noted that during rain periods, water began to accumulate in small pits that were formed between contiguous spoil piles. The spoil material that come out from the interbedded soil material in the lignite sequence and the soft formations removed from the overburden benches.

The material was deposited without deposit pre-qualification at certain selective places. This process excludes the horizontal formation and relatively homogeneous layers as happens in nature. Thus, difficulties started to appear in the assessment of the soil mass with respect to the typical geotechnical and hydraulic parameters. Also,

during the deposition of the first stage, fine grained materials with reduced friction angle and high moisture content, roll over and settled in the gully (Fig. 4.3).

They developed a clay-like base of the waste dump, with high water content. This assumption is supported by past references that state short term stability problems took place during the initial stage of deposit. During that course of time, the waste disposal materials were flowing in relatively large distances from their deposition point, subsequently a stability berm was built along the base of the deposit using pre-selected materials assuring by this way quality [Steiakakis et al., 2009].

During the period of 1982-90, a second deposition phase was designed and implemented, using materials of similar characteristics from the previous deposition, presenting a height of 30-40 m after completion. The dump mass achieved an altitude of +870 to +880 m. Finally in 2004, a third phase of deposit was begun in the central region of the deposit. An addition of 40 meters of material was added, using the stacker A7 (Fig. 4.0). The waste dump registered a height of 100-110 m, leading to an altitude of approximately +910m, while the mean of the overall dump slope was around 5.8°. At the same time, the other two stackers (A6 and A5) were operating on the first and second phase of deposit (Fig. 4.0), at a distance 1.0 and 1.5 km, respectively [Steiakakis et al., 2009].

4.3 DESCRIPTION OF THE FAILURE AT EXTERNAL DUMP DEPOSITION

The failure begun on 30 April 2004, after the deposition of the third phase, showing cracks at the stacker A7 operational level (Fig. 4.0). The cracks were presented parallel to the axis of belt conveyor TD 153. Later on, new cracks were noticeable in the operation level of belt conveyor TD 142 (second stage of deposition), as a result of the traverse ridges which occurred at this location. Gradually, the failure expanded backwards to North-East, presenting a retrogressive failure mode. Then, displacements occurred at the level of the belt conveyor TD 141 (first stage of deposition) as well as at the level of the belt conveyor TD 85, which was operating along the foot of the mass, carrying ash from a very near Power Station to the face of the deposit [Steiakakis et al., 2009].

Site observations showed that individual units had faced downward movements (Fig. 4.1). They moved without particular relative movements, pointing that the sliding surface developed at the base of the deposit. As mentioned previously, materials with low shear resistance had been placed in this zone. The stability of the slope was monitored by measuring the distance between a fixed point and a few monitoring stations (18) installed and distributed in various locations on the slope [Steiakakis et al., 2009].

Based on information shared by mine personnel, almost no movement had been logged until the beginning of the slide. Continuous and systematic monitoring of the

dump was implemented in May 2004 with the purpose of identifying the location, the dimensions and size of the inhibitory dam that was constructed at the toe of the slide with the intention to effectively stop the displacement of the mass [Steiakakis et al., 2009].

Distance logs were taken per hour (on a daily basis) by stations in place. Displacement data were plotted in two ways:

i) Cumulative displacements versus time;
ii) Displacement rate (velocity) with respect to time.

The directions and magnitudes of the movement of each individual monitoring station (with focus on horizontal displacement versus time) were checked by experienced personnel.

In the initial phase, the failure had a moving face velocity of 40-50 m/day (presenting characteristics of a rapid slide) after the construction of inhibitory dams, the motion rate decreased remarkably (10 m/day) and stopped after two months.

Figure 4.4 presents the rate of the movement (in m/day) from May 10 up to July 15, 2004 when all motion practically stopped. It refers to the measurements of the distance between the stable point and a target that is located near the belt conveyor TD 142 [Steiakakis et al., 2009].
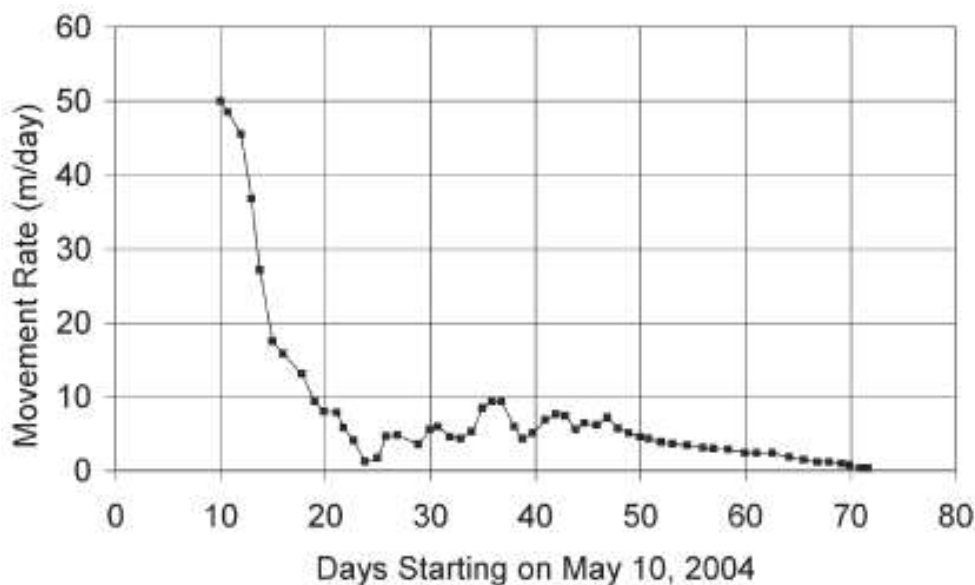

Figure 4.4: Motion rate (between May and July 2004) of a tracking
Station mounted on centre of the sliding mass [Steiakakis et al., 2009].

4.4 GEOLOGY AND HYDROGEOLOGY OF THE LOCATION

In the area where the waste dump is located, the underlying strata is composed of Pliocene–Pleistocene formations (clays, marls, mudstones, marly limestones, breccia and also conglomerate) as well as Quarternary deposits (aged and newer alluvial deposits, fans, talus cones and scree). A cross-section in a direction parallel to "Charavgi's" stream, in which the dump was set, is presented in Fig. 4.5. This section is modeled on qualitative evaluations of geological map information, boreholes data and also general observations at location. The surface of the foundation of the waste dump and the dips of underlying strata are approximately horizontal [Steiakakis et al., 2009].

In relation to hydrogeology, the formations found in place can be characterized by low discharge springs from the contact between the clay formations and the old and new terrestrial deposits. In the place where the instability occurred, a spring of low discharge was present in Charavgi stream (presenting an altitude of +765 m). It was an alternate spring and when the waste dump was started, it was not appraised totally [Steiakakis et al., 2009].

It is important to mention that after the instability, a water discharge with a magnitude greater than 35-40 m3 / h had been watched (June 2004), at a distance between 200-220 m downstream from the site (i.e. in elevation between +770 m and + 780 m). At first, the water presented a muddy appearance, becoming clear after a period of 20 to 30 days. According to the characteristics presented by the outflow, the water would be the result of the process of consolidation of the clayey materials of the soil matrix and also the discharge of the aquifer in the conglomerate formation that underlies the deposit [Steiakakis et al., 2009].

The most probable area where the aquifer of the underlying conglomerate enters in hydraulic contact with the waste dump mass, seems to be on the place where the spring flows out (+763m), and the wider zone with higher elevation, where transverse cracks and ridges had been detected during failure.
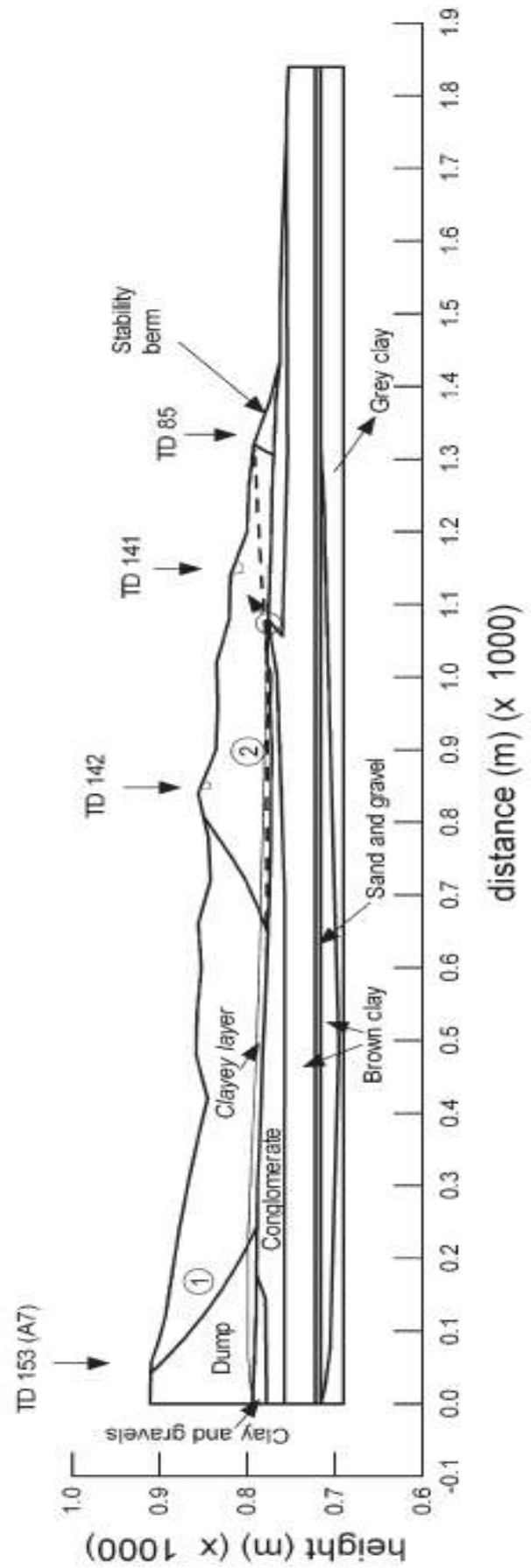
Figure 4.5: Longitudinal view of waste dump [Steiakakis et al., 2009].

Moreover, the area above the failure, accordingly with well data (boreholes YE2 and YE3) the water table is at +833 m during the summer term. During this period, water table in the region downwards of the slide is recorded at elevation between +775 m and +761 m (boreholes YKNP2, EANP1) (Figs. 4 and 4.6). Relying on the water column height of 72 m, which represents the difference between levels, a hydraulic load of 720 kPa is predicted to be charged on water bearing conglomerate formation which underlies the waste dump [Steiakakis et al., 2009].

However, considering the fluctuation of the water table level in the karstic region uphill the instability, which can reach a range of 30 m amongst winter and summer term, the uppermost static water level (Well YE2) is forecast at +863 m. This results in a hydraulic head equal to about 100 m at the spring location (Fig. 4). This pressure was applied in the waste dump before failure, and developed a pore water pressure to 1000 kPa by the end of winter 2004 [Steiakakis et al., 2009].
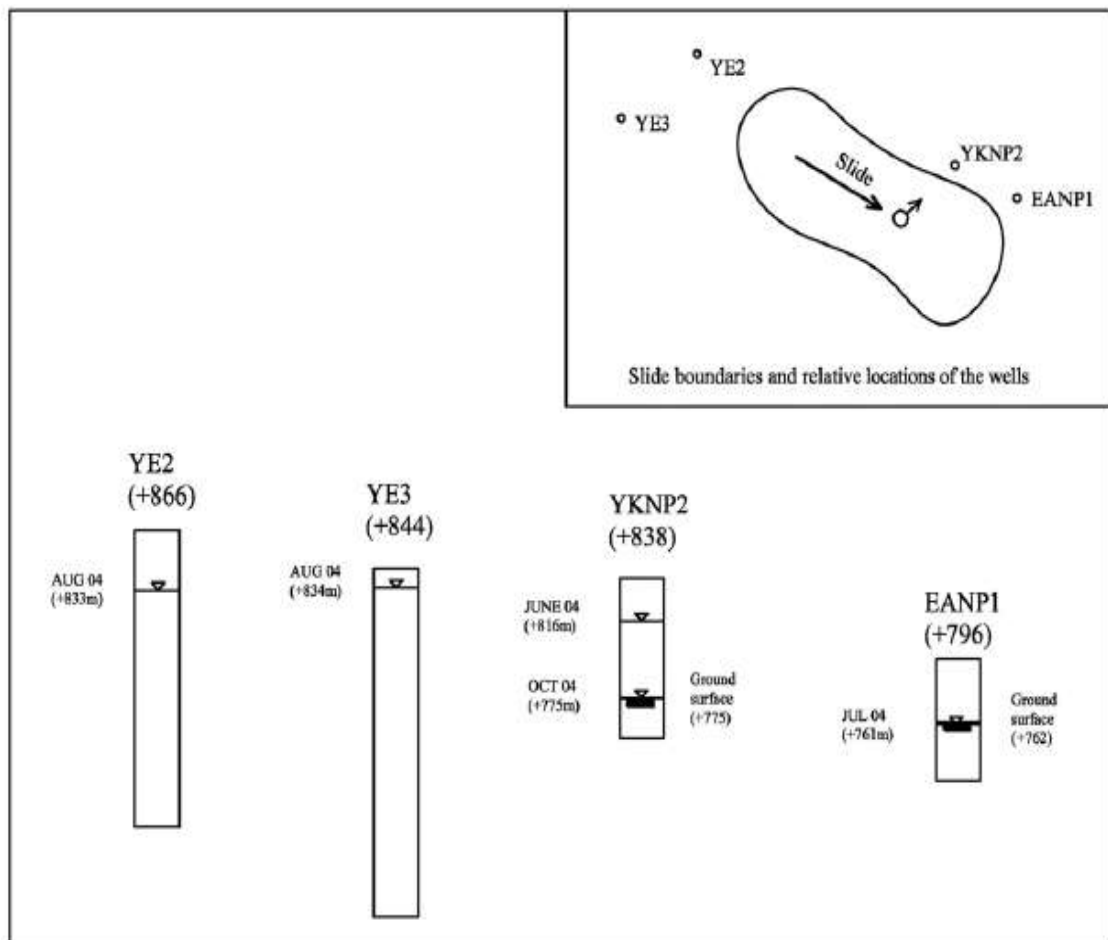
Figure 4.6: Wells & piezometric levels on instability area [Steiakakis et al., 2009].

CHAPTER 05 Analysis and Results

5. NUMERICAL MODELLING
5.1 GEOMETRY

Numerical modelling of the waste dump deposition was carried out on the cross section presented in Fig 5.0 and 5.1. The model was designed considering that the waste material was deposed over ground surface in three phases. The final geometry arrangement and the finite-element mesh applied in the assessment are presented in Fig. 5.2.
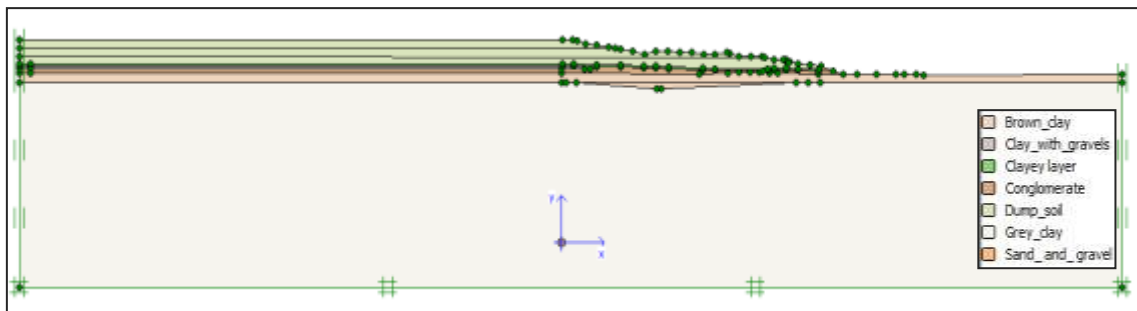

Figure 5.0: Waste dump - Geometry and boundary conditions overview.
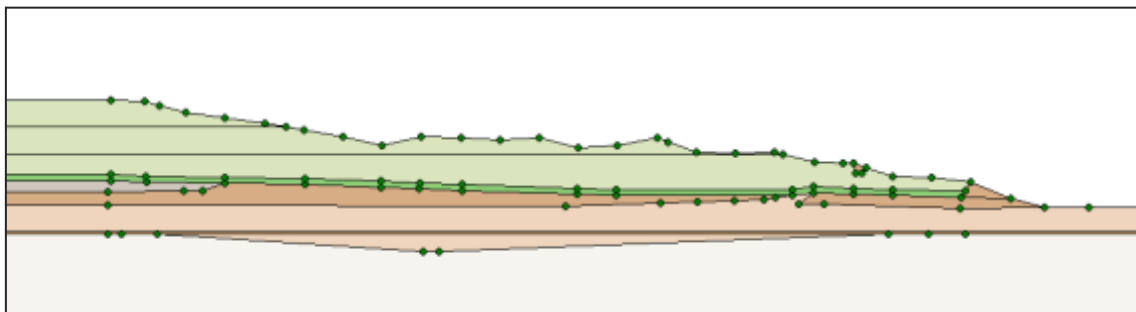
Figure 5.1: Waste dump - Cross section oriented in the direction of movement.

5.2 MODEL MATERIAL PROPERTIES

The Mohr-Coulomb constitutive model as well as the Soft soil model was employed to access the response of the dump material. The geotechnical parameters for every single geological formation as well as waste material modelled in the simulation are shown on Table 4.

Table 4 - Geotechnical properties of the materials applied in both scenarios [Steiakakis et al., 2016].

	Parameter	Dump soil	Clay with gravels	Conglom erate	Brown Clay	Sand and Gravel	Grey clay	Clayey layer
	Models	**MC**	**MC**	**MC**	**MC**	**MC**	**MC**	**MC**
Scenario 1	Unit weight γ (kN/m^3)	19	19,4	18,5	19,4	18,5	18	19
	Young modulus E (MPa)	150	200	250	200	150	450	150
	Poisson ratio ν	0,35	0,49	0,35	0,499	0,35	0,499	0,35
	Cohesion c (kN/m^2)	13,5	16	50	16	10	20	53
	Friction angle ϕ (°)	23,4	24,7	38	24,7	32	35	0
	Permeability K (m/day)	0,086	0,086	8,6	0,009	0,860	0,009	0,086
	Models	**MC**	**MC**	**MC**	**MC**	**MC**	**MC**	**SSM**
Scenario 2	Unit weight γ (kN/m^3)	19	19,4	18,5	19,4	18,5	18	19
	Young modulus E (MPa)	150	200	250	200	150	450	-
	Poisson ratio ν	0,35	0,49	0,35	0,499	0,35	0,499	-
	Cohesion c (kN/m^2)	13,5	16	50	16	10	20	53
	Friction angle ϕ (°)	23,4	24,7	38	24,7	32	35	0
	Permeability K (m/day)	0,086	0,086	8,6	0,009	0,860	0,009	0,086
	Advanced Parameters							
	Mod. Compression index λ^*							0,03
	Mod. Swelling index k^*							0,012

The determination of the properties was based on the technical report for the dump deposit plan. The determination of the geotechnical parameters involved a few uncertainties due to the problems related to heterogeneity, sampling and lab assessment. As a result, their acceptance needs to be handled with care [Steiakakis et al., 2016].

Preceding the input of the material properties, a finite element mesh was made by the Plaxis computer software utilizing 15-node triangular elements. The model had been created to extent below the toe and away from the crest of the slope in order to lessen the effect of the boundary conditions for each model that was analyzed [Steiakakis et al., 2009]. The generated mesh with the 15-node elements was considered capable to offer an effective analysis. The vertical boundaries fixed in the horizontal direction as well as the bottom boundary were fixed in both directions considering that the foundation of the dump is stiff enough. The generation of the initial pore water pressure was based on the piezometric level before the starting of deposition, while subsequent values were determined relying on the development of the waste dump. As previously pointed out, the hydraulic pressure of the underlying aquifer is transmitted in the waste overburden dump and, therefore results in the building up of pore water pressure in the dump deposit [Steiakakis et al., 2016].
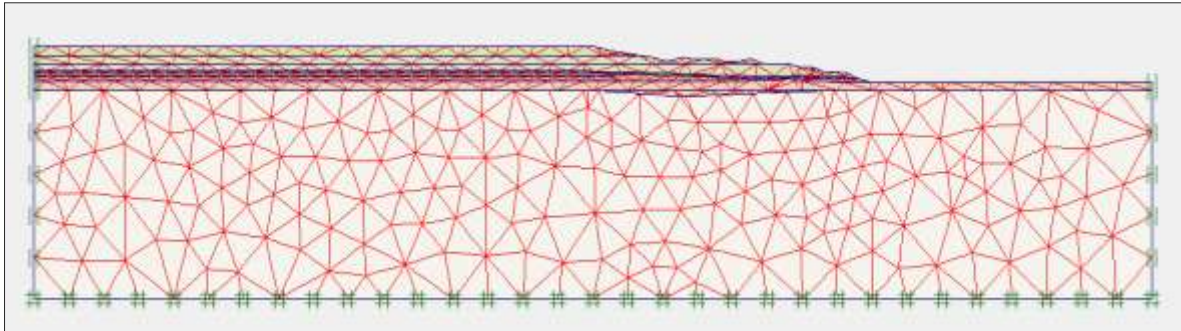
Figure 5.2: Initial mesh and boundary conditions considered on model.

5.3 WATER SETTINGS

As for the water conditions in the soil mass, two different study cases were considered. In the first case an unconfined aquifer was consider present and a second case the existence of an underground Flow.

5.3.1 STUDY CASE 1 – UNCONFINED AQUIFER

In order to understand the effects of depositions in the clayey layer we assume an unconfined aquifer to be present, with a water table near the surface at 790 m (Fig. 5.3). This case assumes relative significance considering that a raise in the water table might notably lessen the factor of safety for a deep failure through the foundation material [Orman et al., 2011].
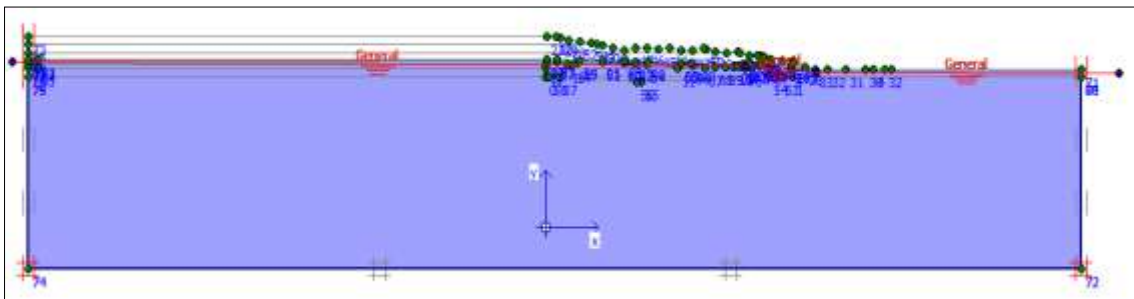
Figure 5.3: Water table at 790m – Study case 1.
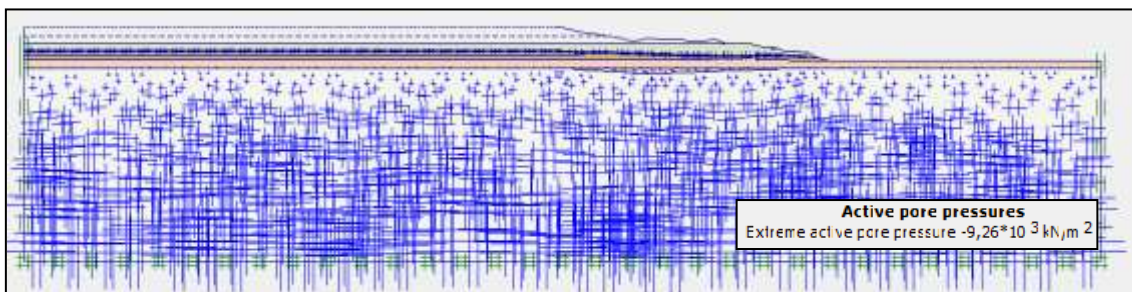
Figure 5.4: Pore pressure distribution in the soil mass – Study case 1.

5.3.2 STUDY CASE 2 – UNDERGROUND FLOW

On this case we consider the existence of an underground flow movement on the conglomerate layer recreating possible winter conditions which is expected to pose a threat to dump stability (Figure 5.5).
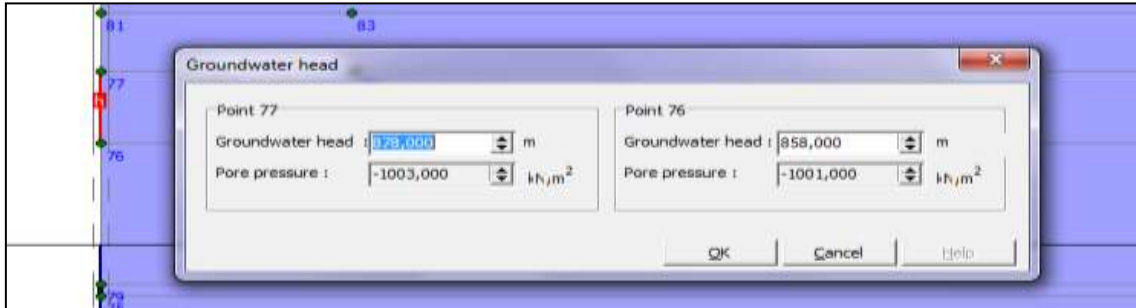
Figure 5.5: Groundwater head selection – Study case 2.

To generate the underground flow (from H to h) on the conglomerate layer, two points were chosen on the model. The first point with higher hydraulic load was created at the edge of the model (Figure 5.5) and the second point (h) was set where it used to exist an intermittent spring (Figure 5.5.1) before the waste dump deposit was initiated. Between both points a hydraulic load equivalent to a water column height of 50 m was selected in order to create enough hydraulic gradient that cause the water to flow along the layer.
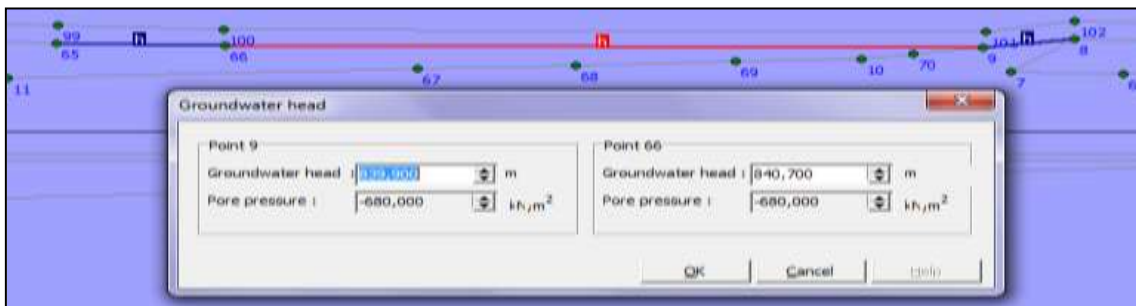
Figure 5.5.1: Groundwater head selection near the spring - Study case 2.

By choosing the option "Generating water pressures" a window appears (Figure 5.5.2) in which the option Groundwater calculation (Steady state) is activated in order to generate water conditions. The Standard settings were chosen by default.
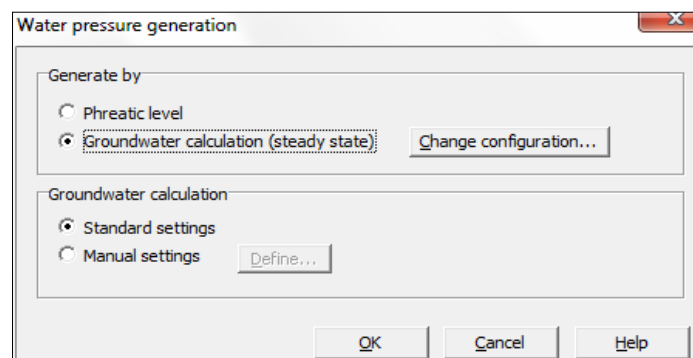
Figure 5.5.2: Water pressure generation - Study case 2.

With this selection Plaxis provide a general view of the water conditions imposed on the soil mass. Subsequently the same procedure was followed for second (Phase 4) and third deposition (Phase 6) layers. Worth to mention that, with the introduction of the third layer (Phase 6) the soil mass collapses.
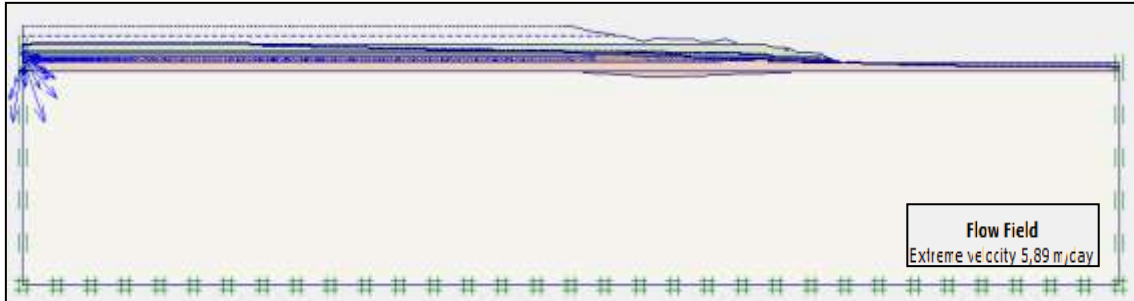
Figure 5.5.3: General view of the underground flow - Study case 2. .

5.4 COMPUTATIONAL PHASES

After defining the boundary conditions, a stage by stage modelling, equivalent to the construction steps concerning the mine dump, was performed. The first stage refers to the initial (gravity) loading of the model, while the remaining stages relate to the sequential activation of adequate mesh clusters in order to replicate the progression of the dump. The "c/φ reduction procedure" was also applied in order to determine the stability factor at each stage of deposition. Following this procedure, slope failure was created by indicating a proper number of loading steps during which the strength parameters φ and c are reduced until failure of the slope occurs [Plaxis, 2012 b].

5.4.1 COMPUTATIONAL PHASES | SCENARIOS

Regarding to material models, two different scenarios were considered and applied on the analysis of both study cases (1 and 2).

5.4.1.1 SCENARIO: 1 | REGARDING MATERIAL MODELS

A first scenario was considered in which the clayey layer was governed by the classic Mohr-Coulomb soil model and to be undrained, whereby the others layers were considered to be drained and governed by Mohr-Coulomb model as well.

5.4.1.2 SCENARIO: 2 | REGARDING MATERIAL MODELS

With respect to the second scenario the clayey layer had been assumed to be dictated by the Soft Soil model, which was considered to be undrained. The rest of the layers were assumed drained and governed by Mohr-Coulomb.
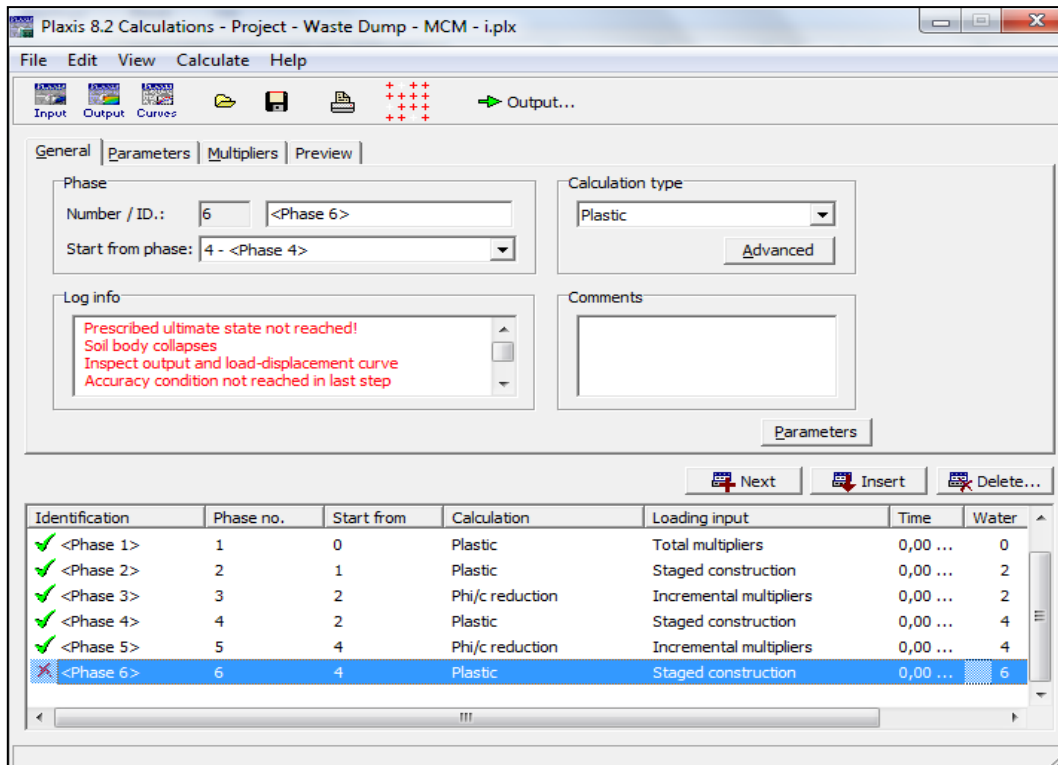
**Figure 5.6:** Computational phases – scenario 1.
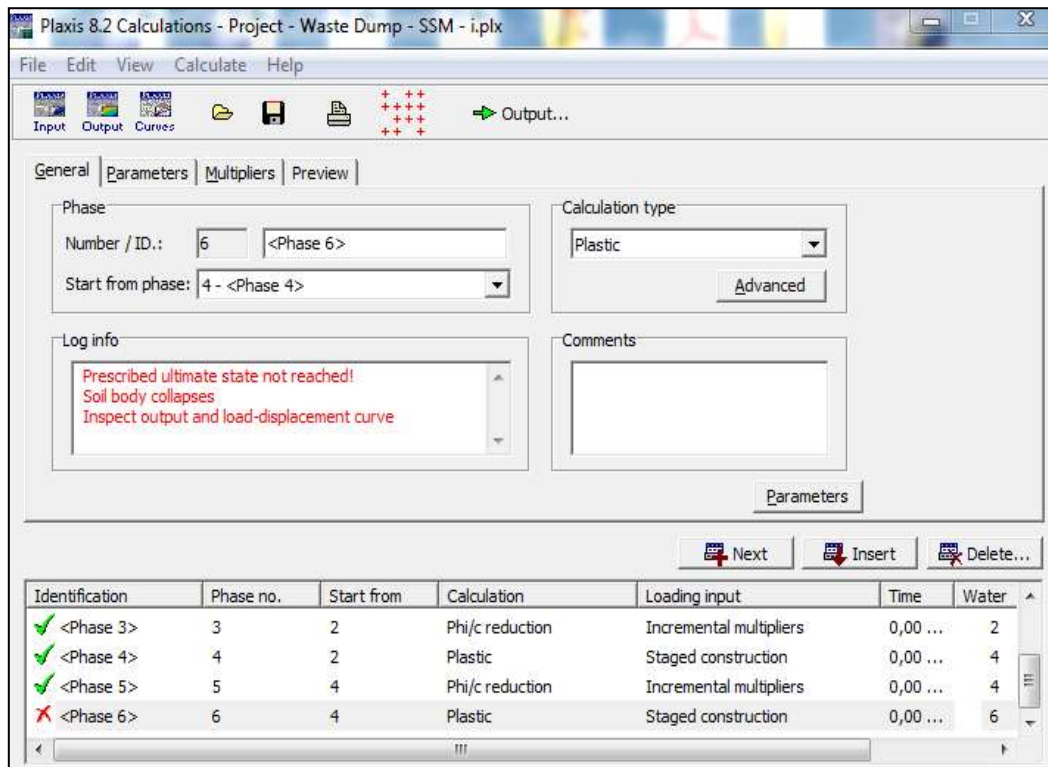
Figure 5.7: Computational phases – scenario 2.

As shown on both figures the soil mass collapses for both scenarios after the third deposition being added. On Table 5, we can find the values of the factor of safety (FS) for both study cases (1 and 2) in each deposition.

Table 5 – Values for factor of safety (FS) on both study cases (1 and 2).

First Scenario – Study case 1 (Unconfined aquifer)	Factor of Safety
1st Stage of deposition	1,2291
2nd Stage of deposition	1,1237
3rd Stage of deposition	-
Second Scenario – Study case 1 (Unconfined aquifer)	Factor of Safety
1st Stage of deposition	1,2587
2nd Stage of deposition	1,1330
3rd Stage of deposition	-
First Scenario – Study case 2 (Underground flow)	Factor of Safety
1st Stage of deposition	1,2279
2nd Stage of deposition	1,1081
3rd Stage of deposition	-
Second Scenario – Study case 2 (Underground flow)	Factor of Safety
1st Stage of deposition	1,2735
2nd Stage of deposition	1,1242
3rd Stage of deposition	-

5.5 RESULTS

In order to understand how soil depositions in conjunction with pore water pressure affect the soil mass and to understand where the displacements would occur, a numerical modelling analysis was conducted supported by computational simulation of geological scenarios. Is worth to mention that the focus was mainly on the clayey layer.

A selection of Plastic points (1), Relative shear stresses (2), shear strains (3), total displacements (4), and excess of pore pressure graphs (5). The first can provide us with the stress points that are in a plastic state in any step in the calculation history, the second can give a sign regarding the proximity of the stress point to the failure envelope which can be very useful in order to understand where and when the failure will occur; the third present the total deformations; on the fourth the Total displacements (Utotal) which provides the different components of the accumulated displacements at the end of each calculation step; the last, the Excess of pore pressure where we can see the result from undrained behaviour and how is affected by stress changes due to loading or a change in hydraulic conditions [Plaxis, 2012 a].

5.5.1 STUDY CASE 1 | SCENARIO 1: REGARDING THE MATERIAL MODELS

<p align="center">1st PHASE OF DEPOSITION</p>

On the first deposition a load of 29 m height of spoil material was added to the soil foundation. This layer material was considered to be drained.
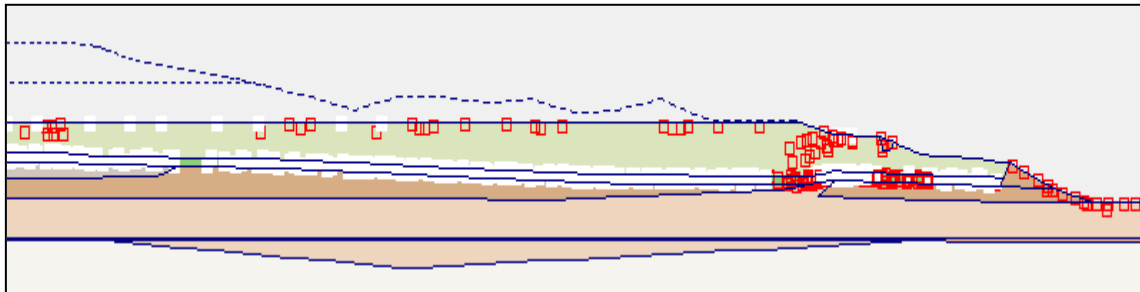
**Figure 6.0:** Distribution of the plastic points after the first deposition – Study case 1 & Scenario 1.
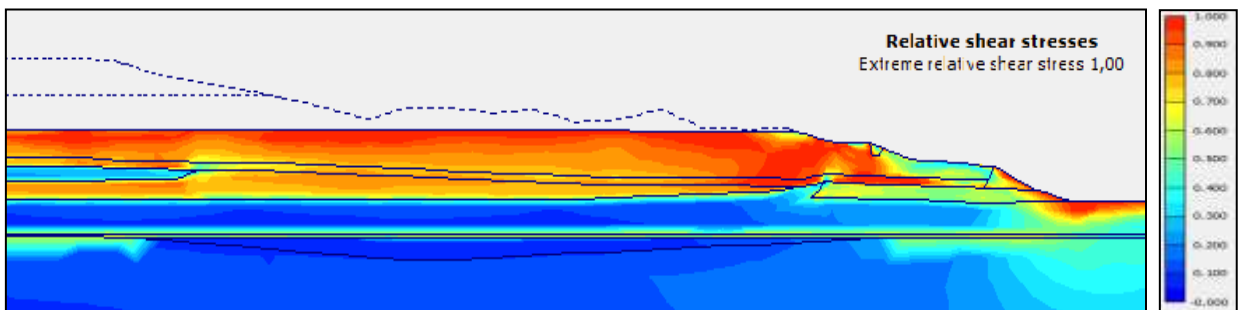
**Figure 6.1:** Relative Shear stresses after the first deposition - Study case 1 & Scenario 1.
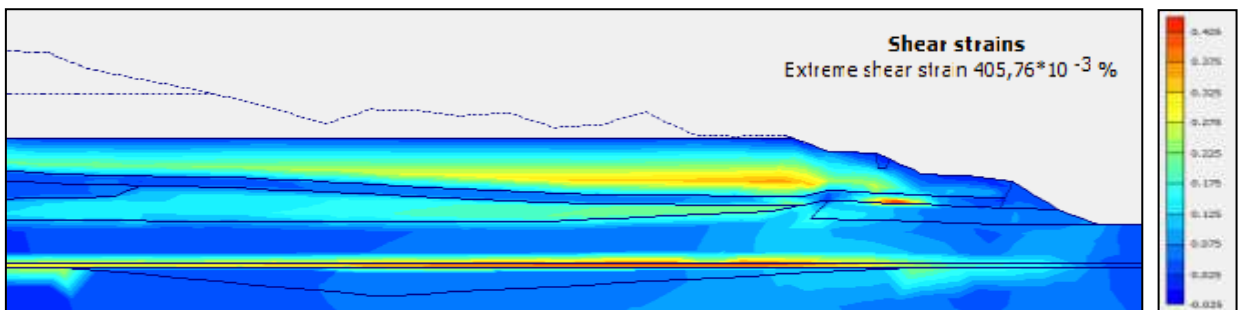
Figure 6.1.1: Shear strains after the first deposition - Study case 1 & Scenario 1.
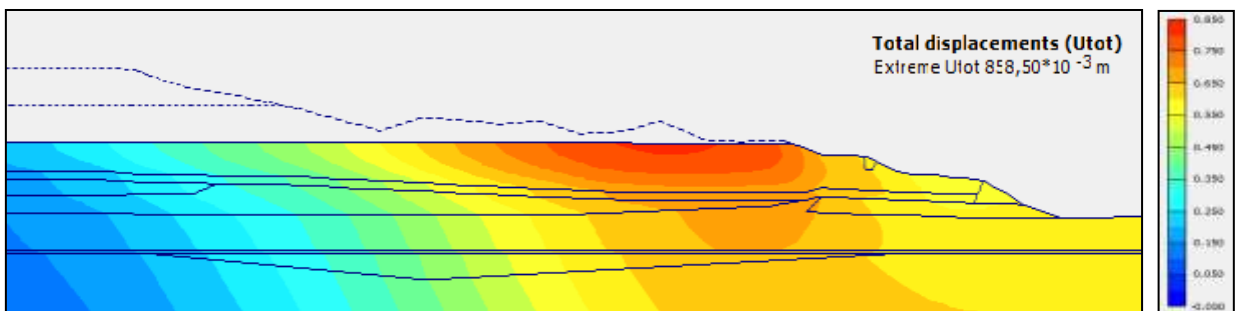
**Figure 6.1.2:** Maximum displacement (Utotal) after the first deposition - Study case 1 & Scenario 1.
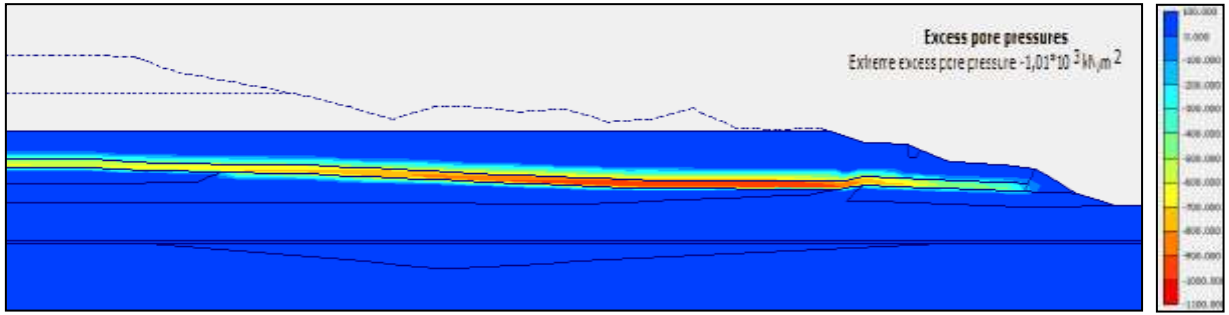
Figure 6.1.3: Excess of pore pressure after the first deposition - Study case 1 & Scenario 1.

2nd PHASE OF DEPOSITION

The second phase of deposition was characterized by adding a new layer of 39 m height of spoil material resulting from the mine exploitation. This new layer was considered to be drained.
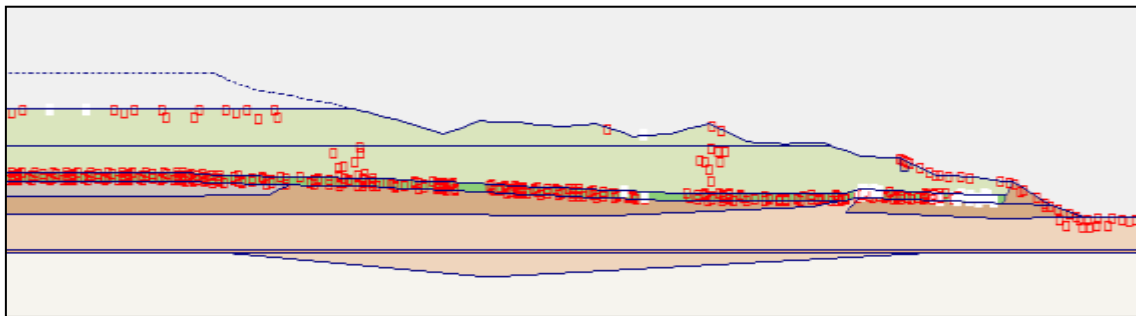
Figure 6.2: Distribution of the plastic points after the second deposition - Study case 1 & Scenario 1.
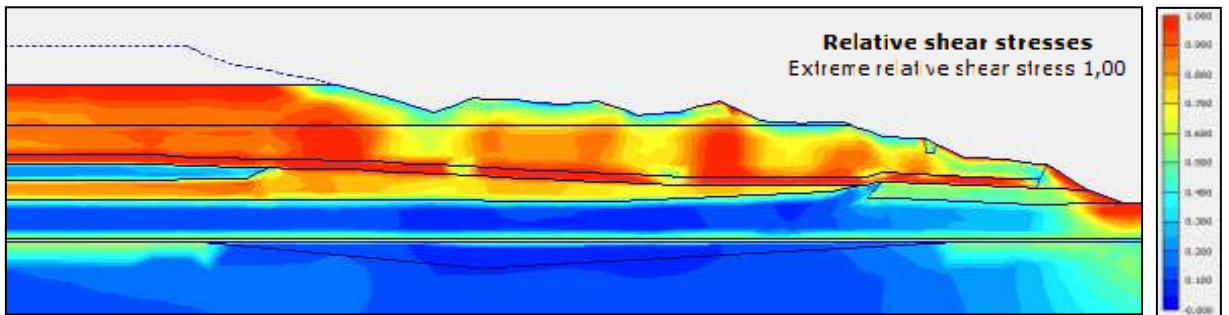

**Figure 6.2.1**: Relative Shear stresses after the second deposition - Study case 1 & Scenario 1.
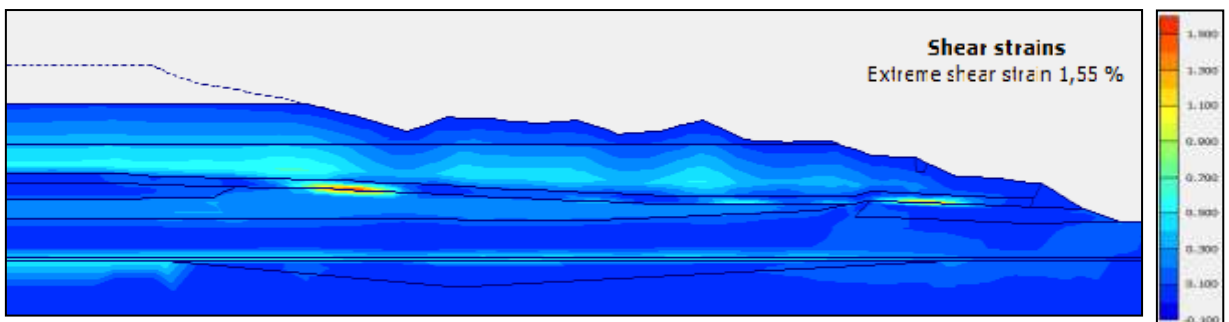
Figure 6.2.2: Shear strains after the second deposition - Study case 1 & Scenario 1.
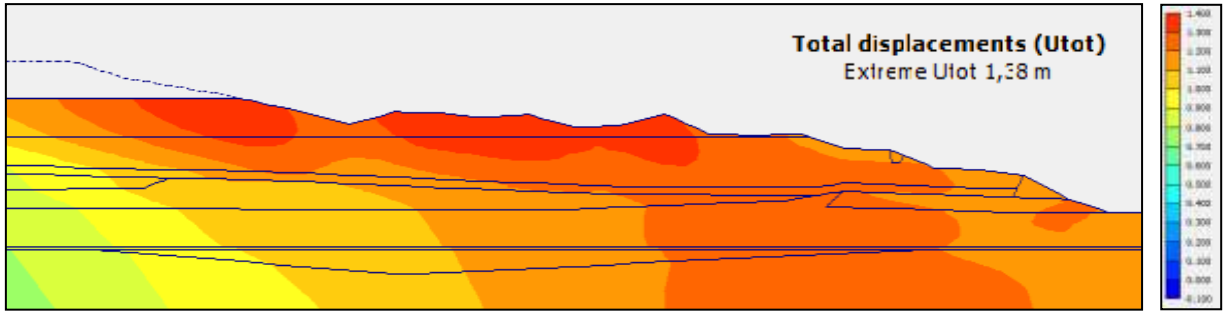
**Figure 6.2.3:** Maximum displacement (Utotal) after the second deposition - Study case 1 & Scenario 1.
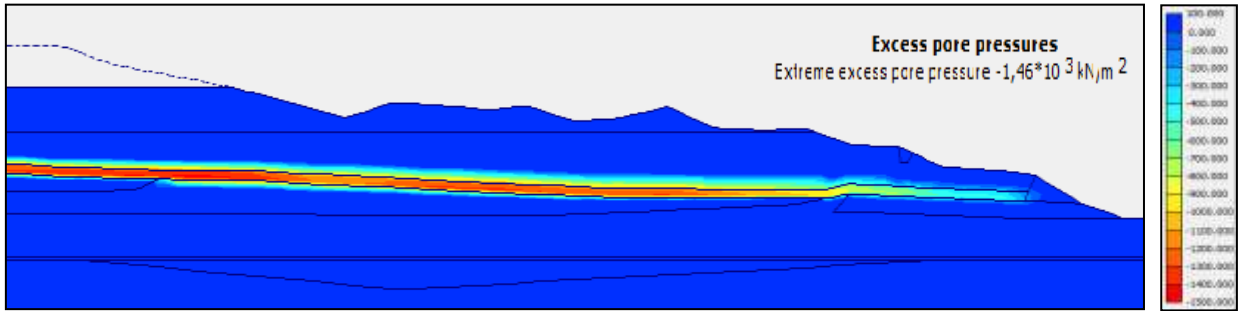
Figure 6.2.4: Excess of pore pressure after the second deposition - Study case 1 & Scenario 1.

<div align="center">

3rd PHASE OF DEPOSITION

</div>

On the third and final deposition a 40 m height of soil mass resulting from mine operations was piled into the existent soil dump. This new layer was considered to be drained.
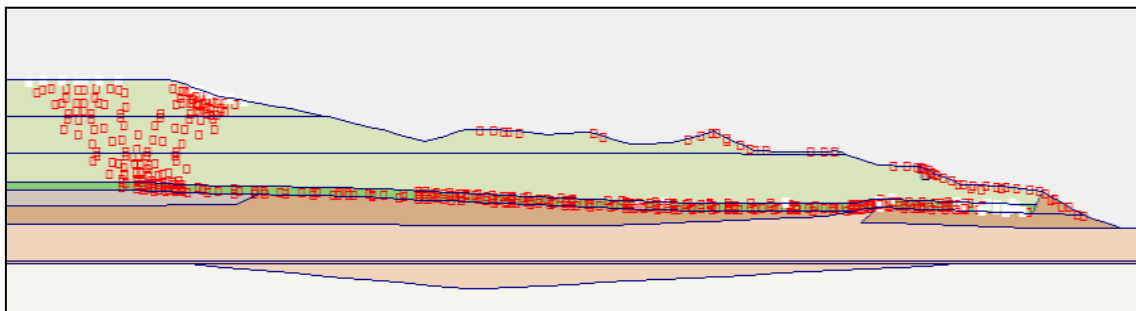

**Figure 6.3**: Distribution of the plastic points after the third deposition - Study case 1 & Scenario 1.
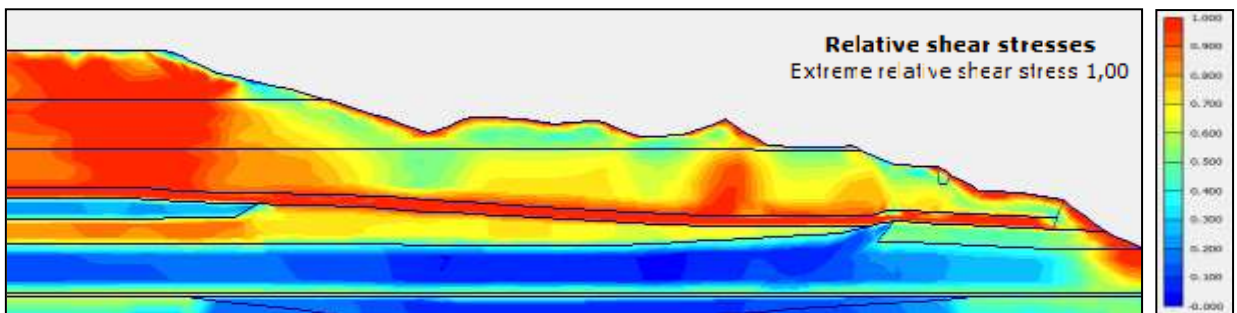
Figure 6.3.1: Relative Shear stresses after the third deposition - Study case 1 & Scenario 1.
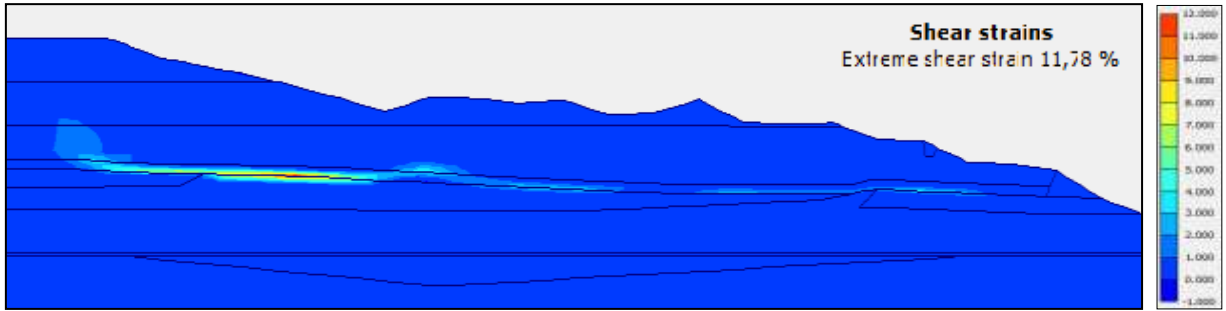
Figure 6.3.2: Shear strains after the third deposition - Study case 1 & Scenario 1.
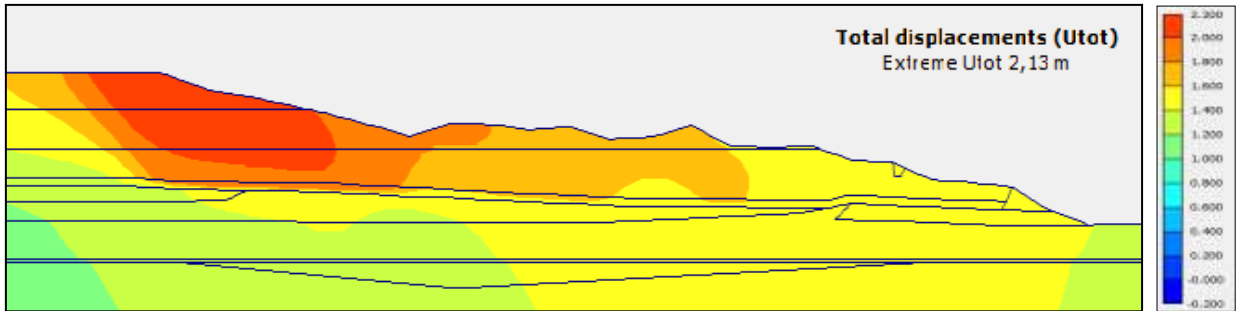
Figure 6.3.3: Maximum displacement (Utotal) after the third deposition - Study case 1 & Scenario 1.
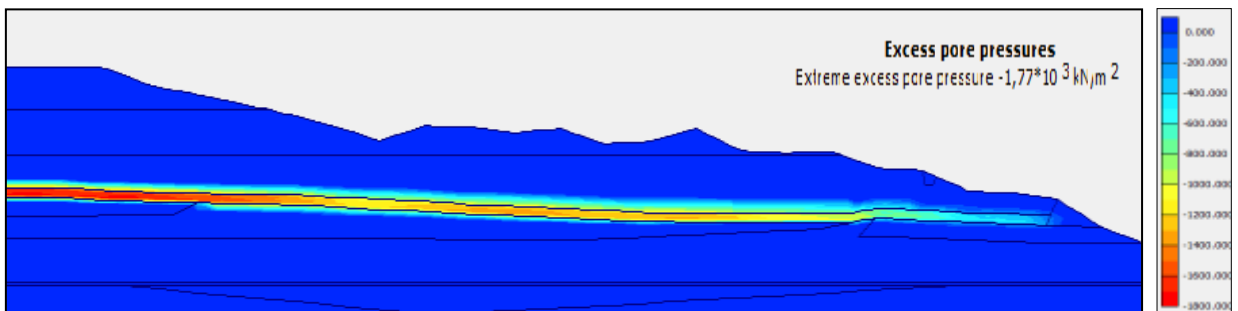
Figure 6.3.4: Excess of pore pressure after the third deposition - Study case 1 & Scenario 1.

5.5.2 STUDY CASE 1 | SCENARIO 2: REGARDING THE MATERIAL MODELS

1st PHASE OF DEPOSITION

On the first deposition a load of 29m height of bulk material was added to the soil foundation. This layer material was considered to be drained.
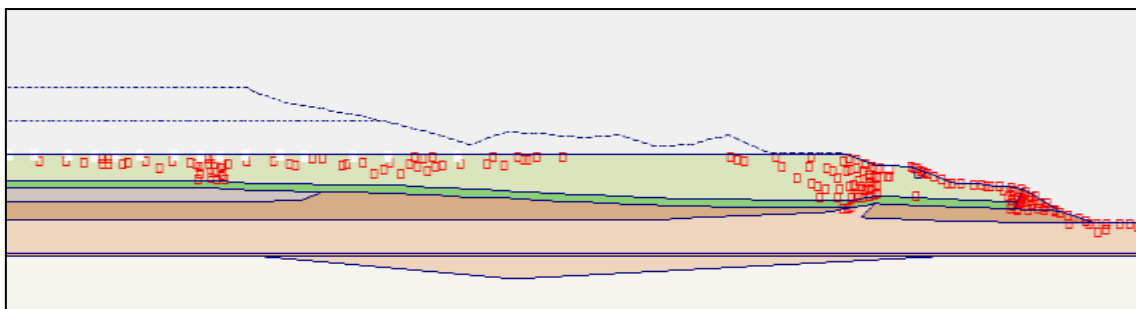
Figure 6.4: Distribution of the plastic points after the first deposition - Study case 1 & Scenario 2.
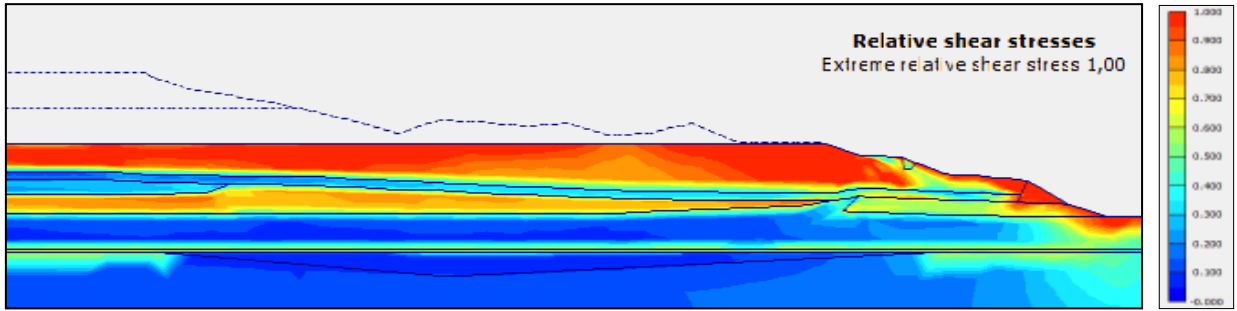
Figure 6.4.1: Relative Shear stresses after the first deposition - Study case 1 & Scenario 2.
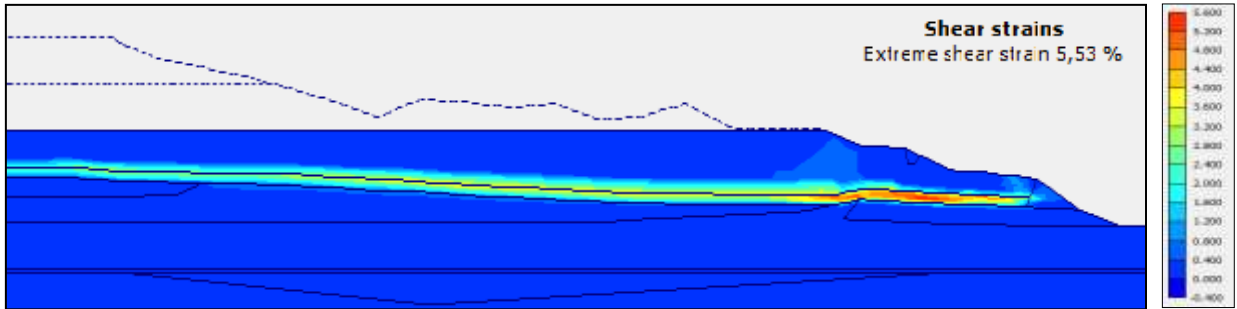

Figure 6.4.2: Shear strains after the first deposition - Study case 1 & Scenario 2.
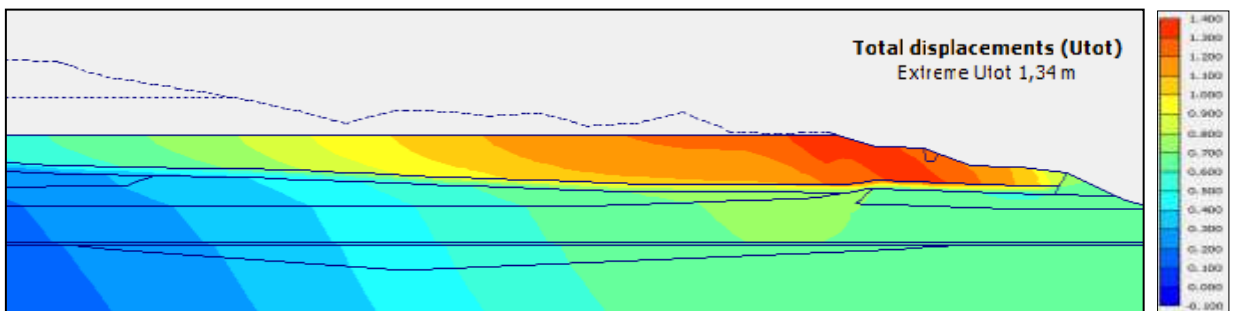

Figure 6.4.3: Maximum displacement (Utotal) after the first deposition - Study case 1 & Scenario 2.
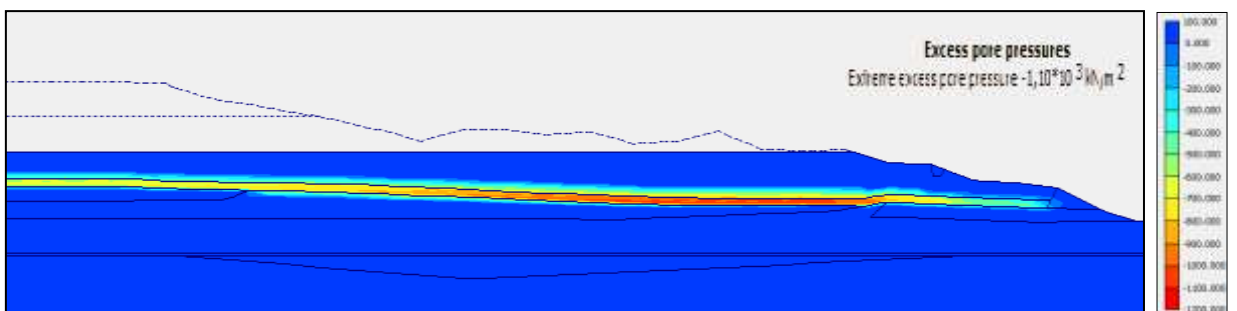

Figure 6.4.4: Excess of pore pressure after the first deposition - Study case 1 & Scenario 2.

2nd PHASE OF DEPOSITION

The second phase of deposition was characterized by adding a new layer of 39m height of spoil material resulting from the mine exploration. This new layer was considered to be drained.
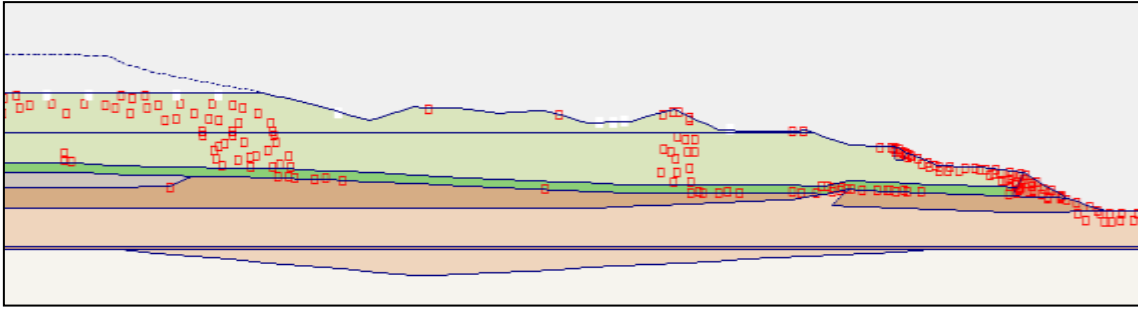
Figure 6.5: Distribution of the plastic points after the second deposition - Study case 1 & Scenario 2.
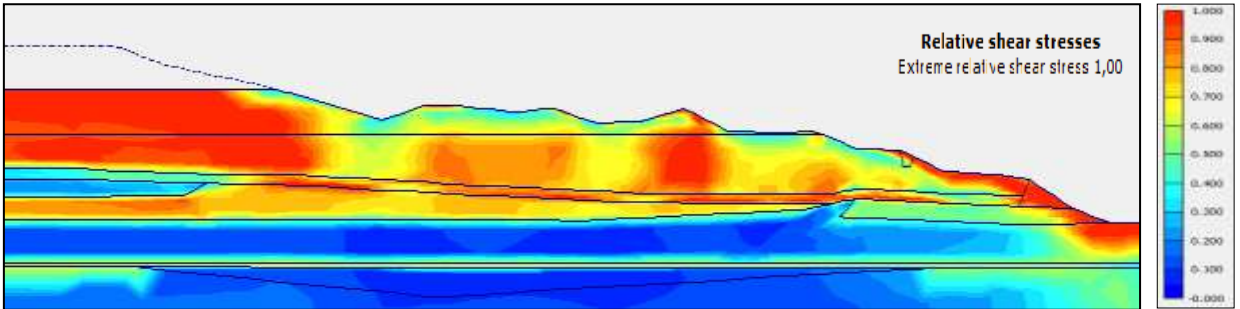

Figure 6.5.1: Relative Shear stresses after the second deposition - Study case 1 & Scenario 2.
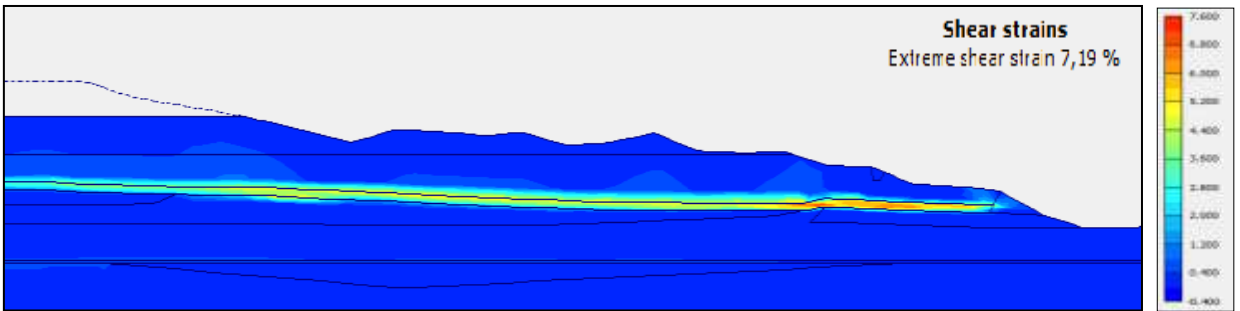

Figure 6.5.2: Shear strains after the second deposition - Study case 1 & Scenario 2.
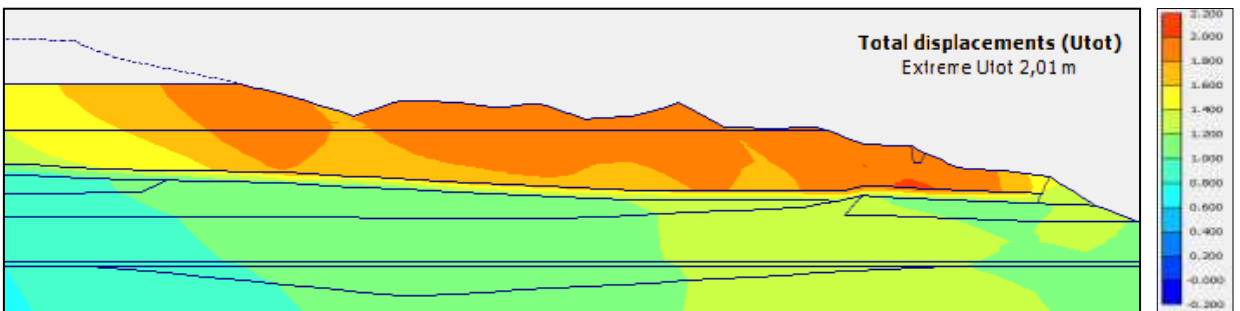

**Figure 6.5.3:** Maximum displacement (Utotal) after the second deposition - Study case 1 & Scenario 2.
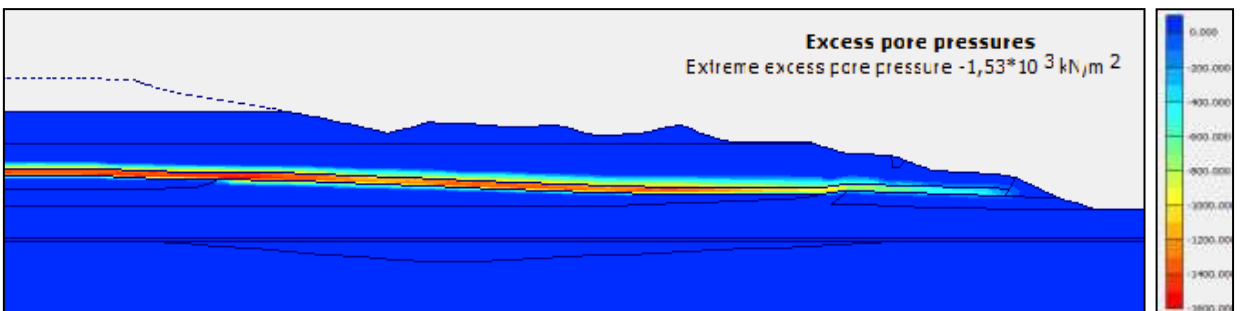
Figure 6.5.4: Excess of pore pressure after the second deposition - Study case 1 & Scenario 2.

3rd PHASE OF DEPOSITION

On the third and final deposition a 40m height of soil mass resulting from mine operations was piled into the existent soil dump. This new layer was considered to be drained.
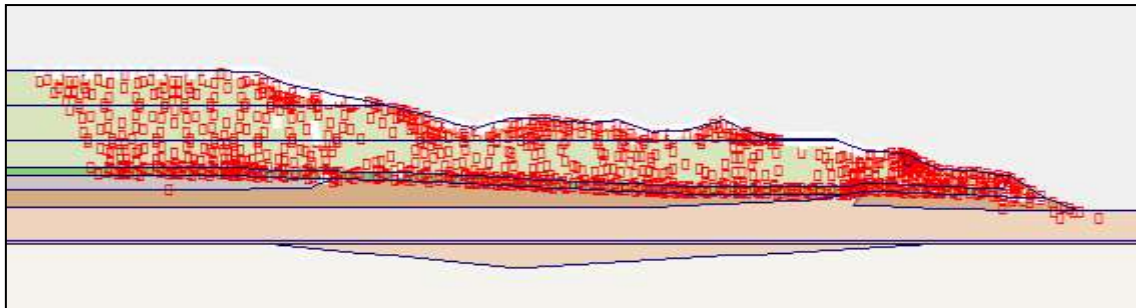

**Figure 6.6**: Distribution of the plastic points after the third deposition - Study case 1 & Scenario 2.
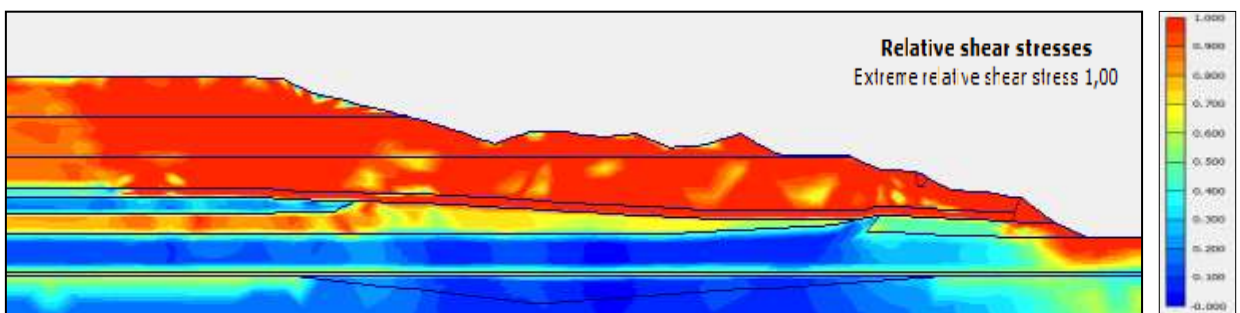
**Figure 6.6.1**: Relative Shear stresses after the third deposition - Study case 1 & Scenario 2.
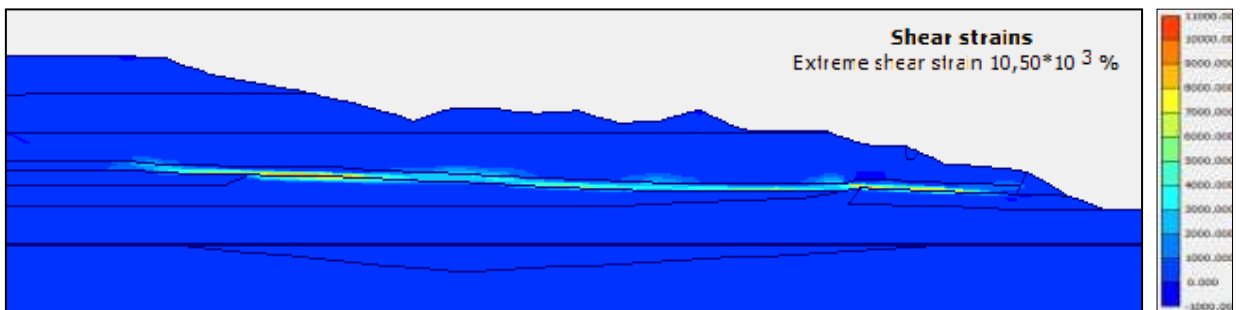
**Figure 6.6.2**: Shear strains after the third deposition - Study case 1 & Scenario 2.
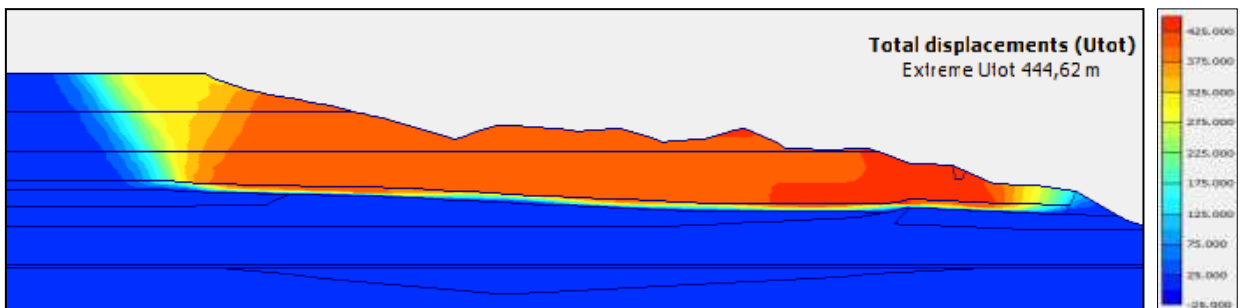
Figure 6.6.3: Maximum displacement (Utotal) after the third deposition - Study case 1 & Scenario 2.
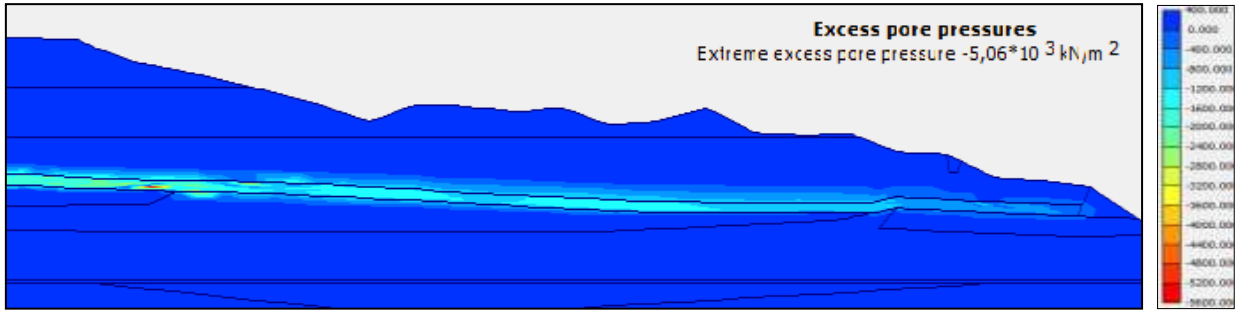
Figure 6.6.4: Excess of pore pressure after the third deposition - Study case 1 & Scenario 2.

5.5.3 STUDY CASE 2 | SCENARIO 1: REGARDING THE MATERIAL MODELS

1st PHASE OF DEPOSITION

On the first deposition a load of 29 m height of bulk material was added to the soil foundation. This layer material was considered to be drained.
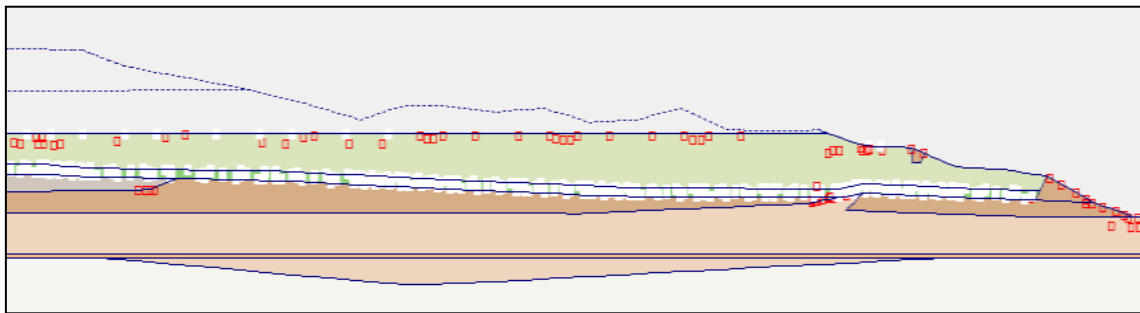

**Figure 6.7**: Distribution of the plastic points after the first deposition - Study case 2 & Scenario 1.
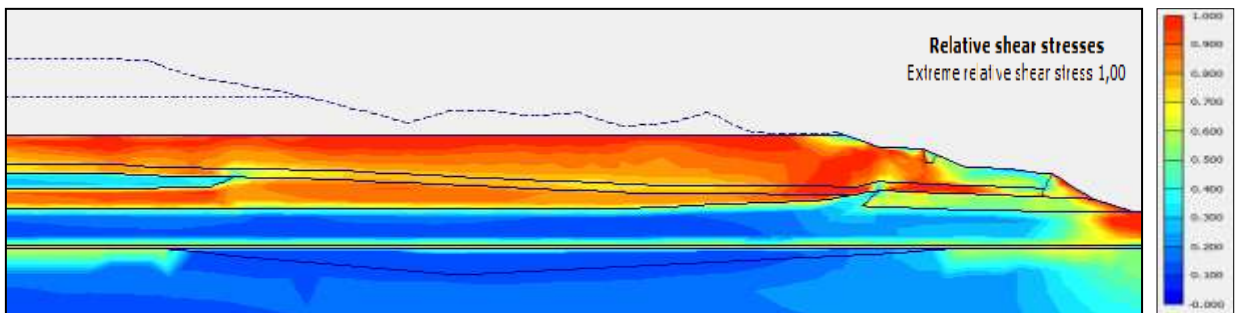
Figure 6.7.1: Relative Shear stresses after the first deposition - Study case 2 & Scenario 1.
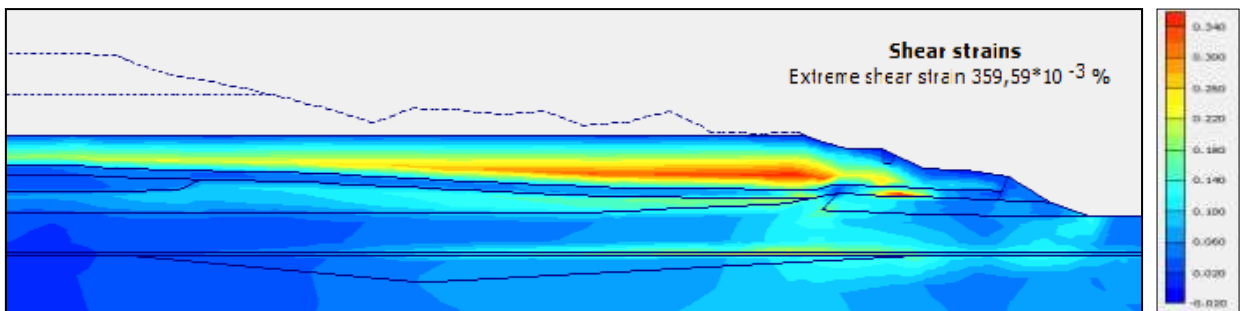
Figure 6.7.2: Shear strains after the first deposition - Study case 2 & Scenario 1.
.
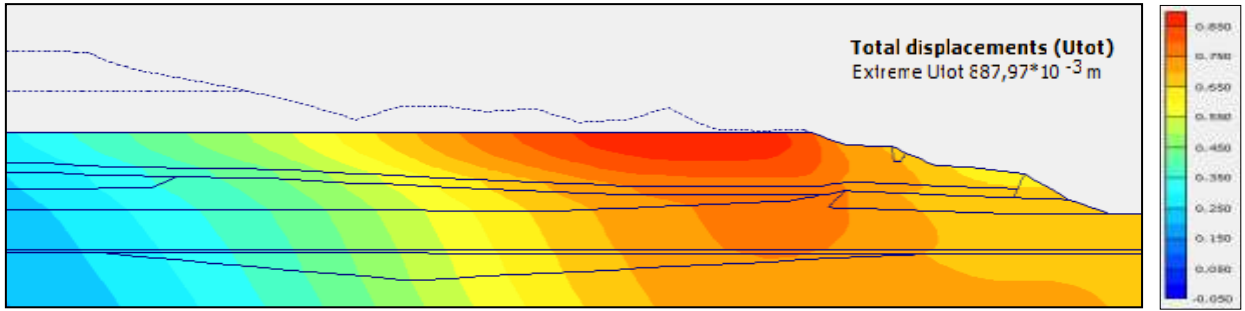
Figure 6.7.3: Maximum displacement (Utotal) after the first deposition - Study case 2 & Scenario 1.
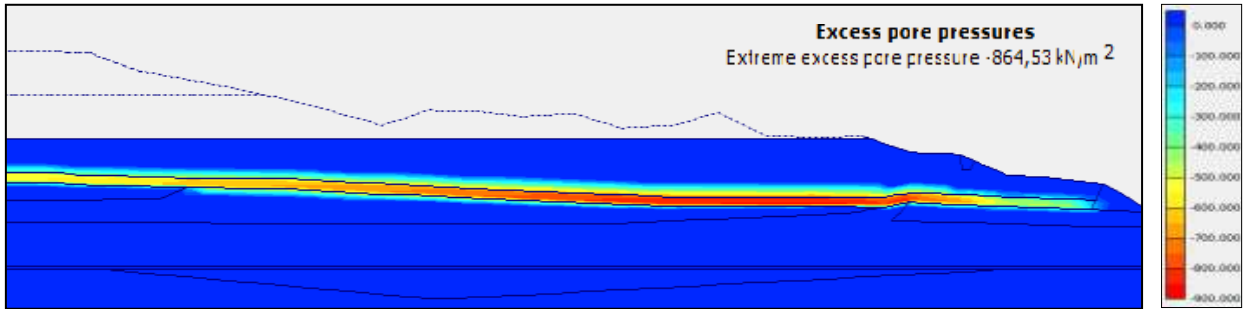
Figure 6.7.4: Excess of pore pressure after the first deposition – Study case 2 & Scenario 1.

2nd PHASE OF DEPOSITION

The second phase of deposition was characterized by adding a new layer of 39 m height of spoil material resulting from the mine exploration. This new layer was considered to be drained.
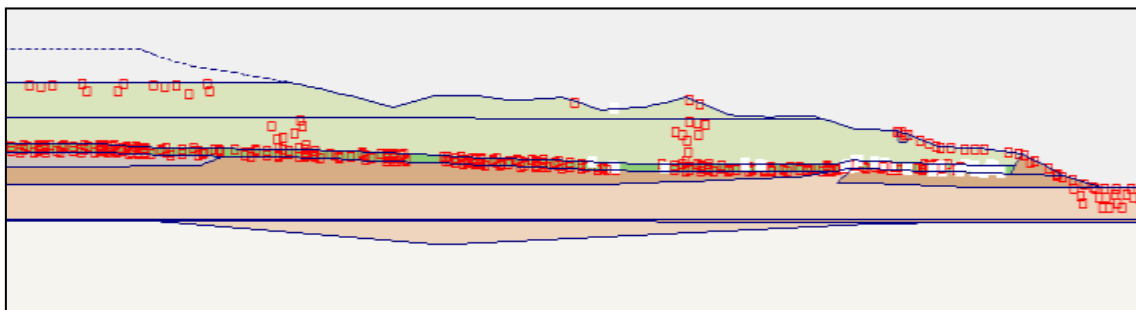
Figure 6.8: Distribution of the plastic points after the second deposition - Study case 2 & Scenario 1.
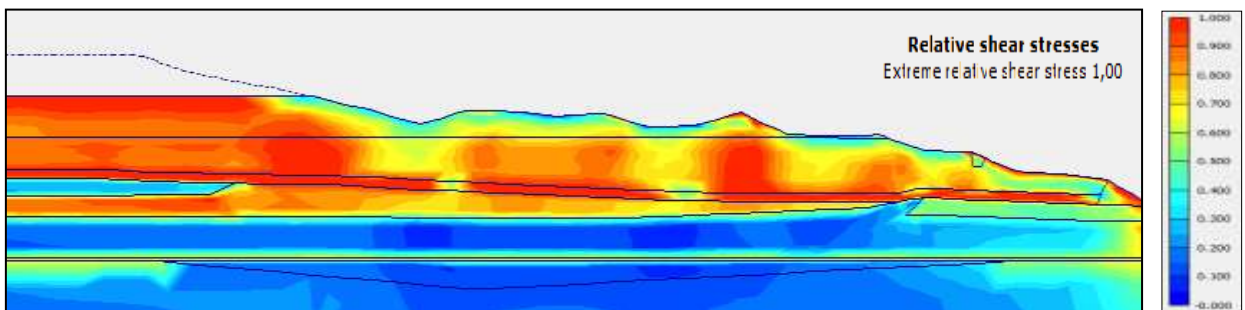
Figure 6.8.1: Relative Shear stresses after the second deposition - Study case 2 & Scenario 1.
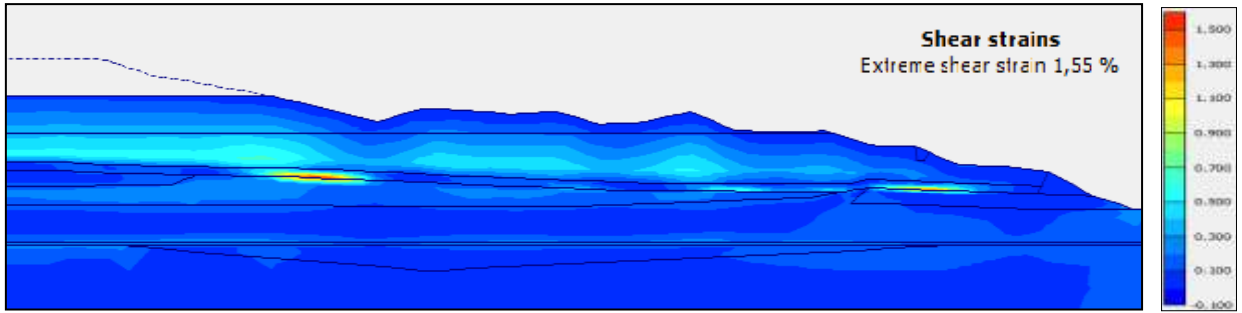
Figure 6.8.2: Shear strains after the second deposition - Study case 2 & Scenario 1.
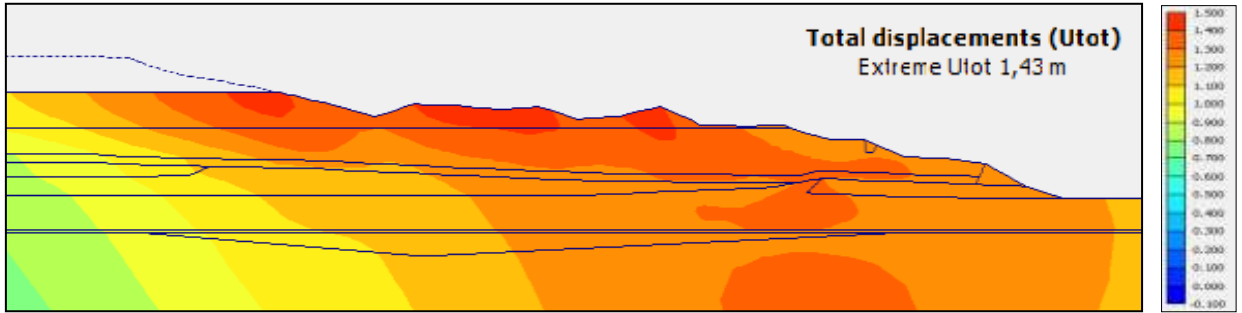
Figure 6.8.3: Maximum displacement (Utotal) after the second deposition - Study case 2 & Scenario 1.
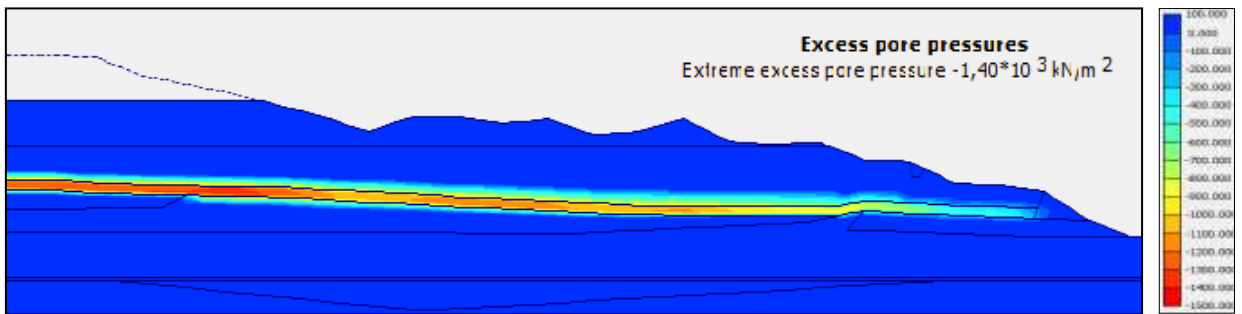
Figure 6.8.4: Excess of pore pressure after the second deposition – Study case 2 & Scenario 1.

3rd PHASE OF DEPOSITION

On the third and final deposition a 40m height of soil mass resulting from mine operations was piled into the existent soil dump. This new layer was considered to be drained.
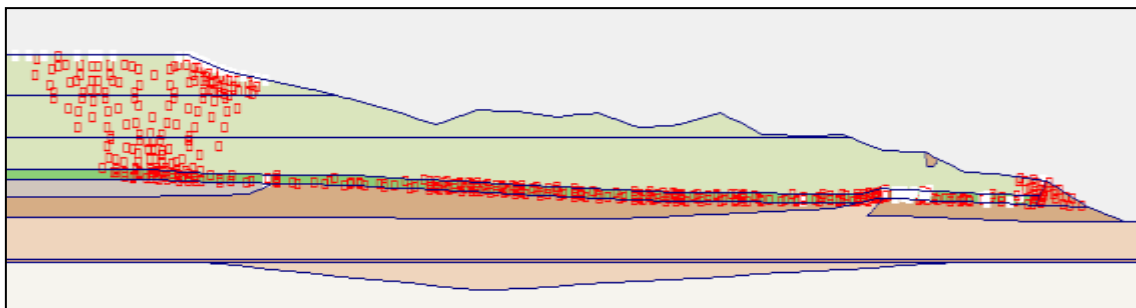
Figure 6.9: Distribution of the plastic points after the third deposition - Study case 2 & Scenario 1.
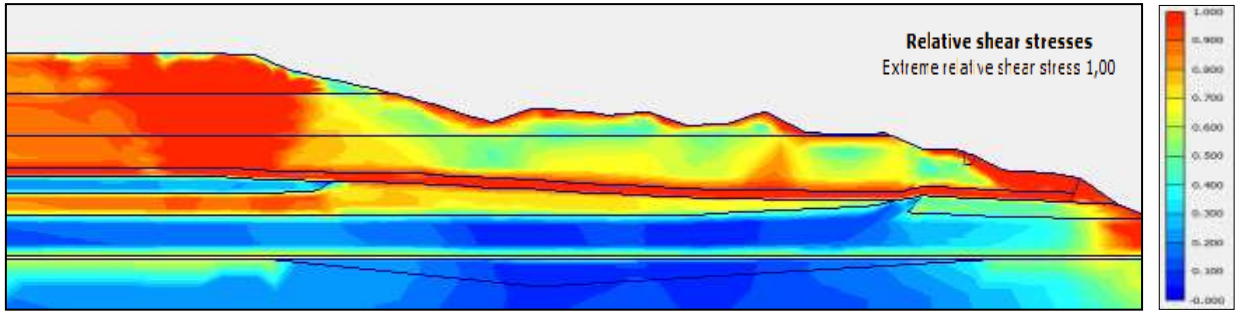
**Figure 6.9.1**: Relative Shear stresses after the third deposition - Study case 2 & Scenario 1.
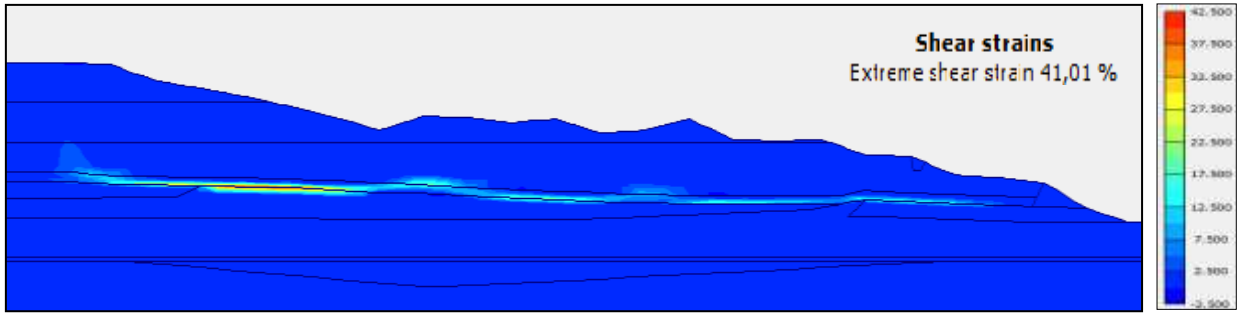
**Figure 6.9.2**: Shear strains after the third deposition - Study case 2 & Scenario 1.
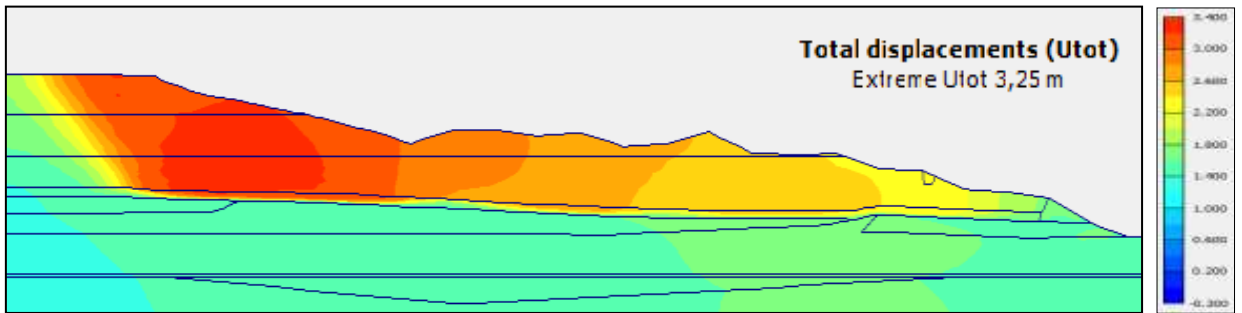
Figure 6.9.3: Maximum displacement (Utotal) after the third deposition - Study case 2 & Scenario 1.
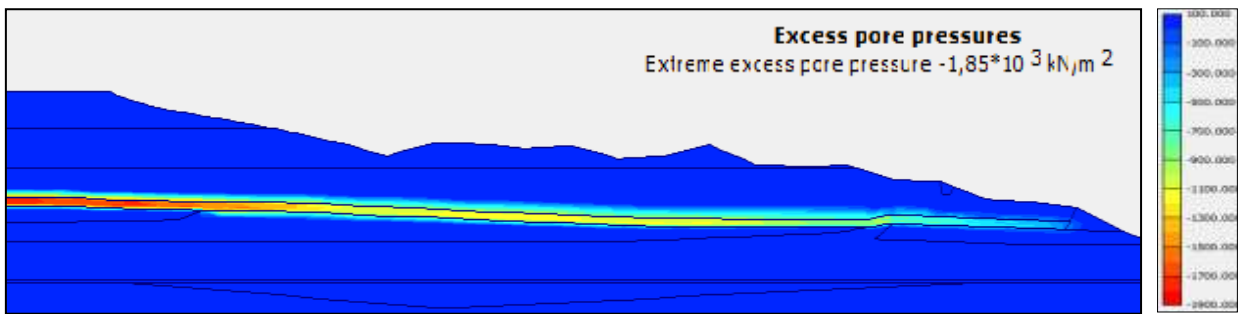

Figure 6.9.4: Excess of pore pressure after the third deposition – Study case 2 & Scenario 1.

5.5.4 STUDY CASE 2 | SCENARIO 2: REGARDING THE MATERIAL MODELS

<p align="center">1st PHASE OF DEPOSITION</p>

A first deposition characterized by a load of 29 m height of bulk material was applied to the soil foundation. This layer material was considered to be drained.
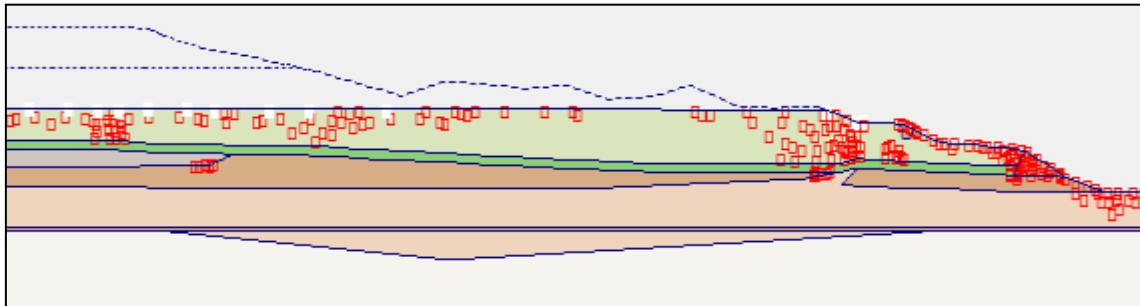
Figure 7.0: Distribution of the plastic points after the first deposition - Study case 2 & Scenario 2.
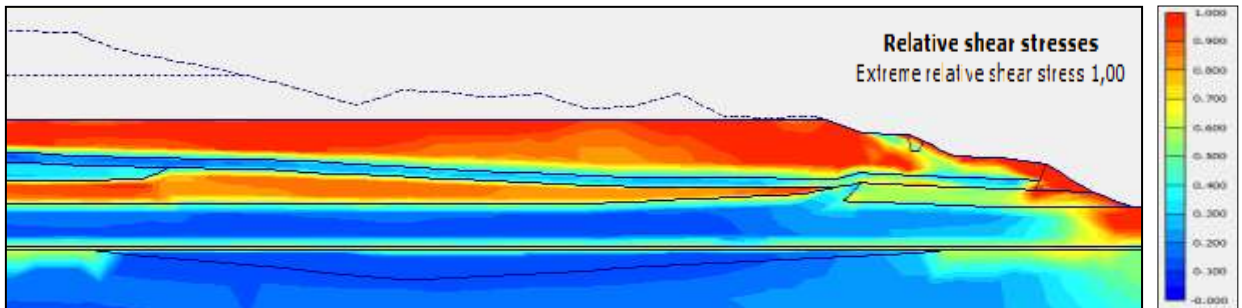
Figure 7.1: Relative Shear stresses after the first deposition - Study case 2 & Scenario 2.
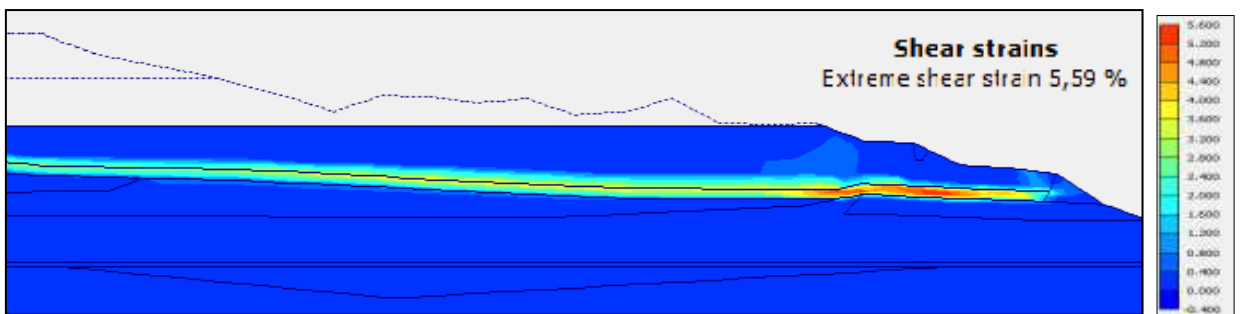
Figure 7.1.1: Shear strains after the first deposition - Study case 2 & Scenario 2.
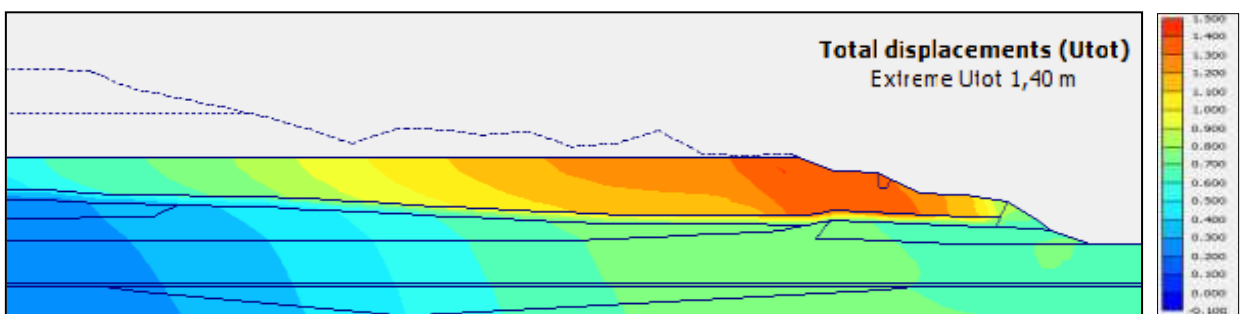
Figure 7.1.2: Maximum displacement (Utotal) after the first deposition - Study case 2 & Scenario 2.
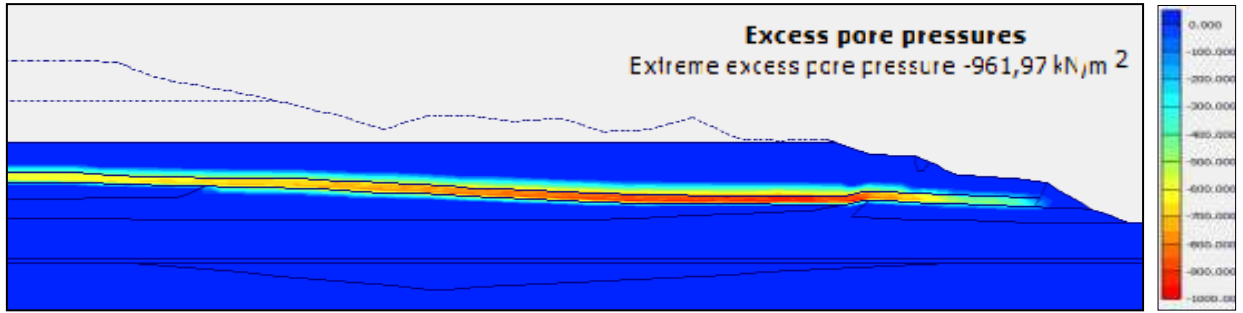
Figure 7.1.3: Excess of pore pressure after the first deposition – Study case 2 & Scenario 2.

2nd PHASE OF DEPOSITION

The second phase of deposition was featured by the sum of a new layer of 39m height of waste material derived from the mine exploitation. Being this new layer considered to be drained.
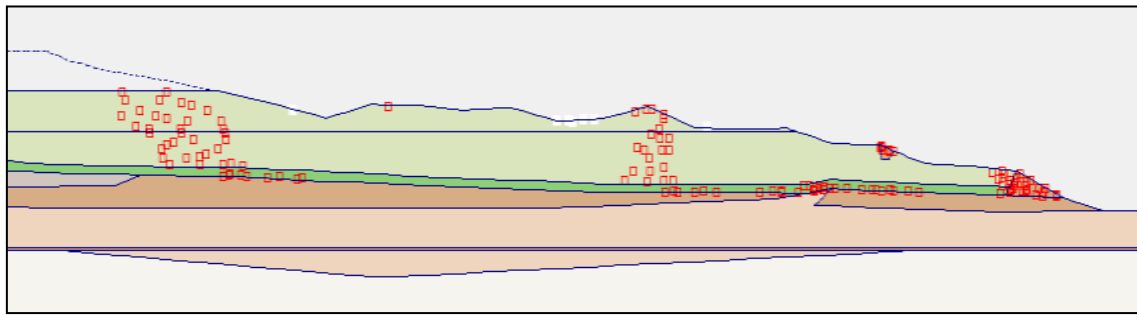
**Figure 7.2**: Distribution of the plastic points after the second deposition - Study case 2 & Scenario 2.
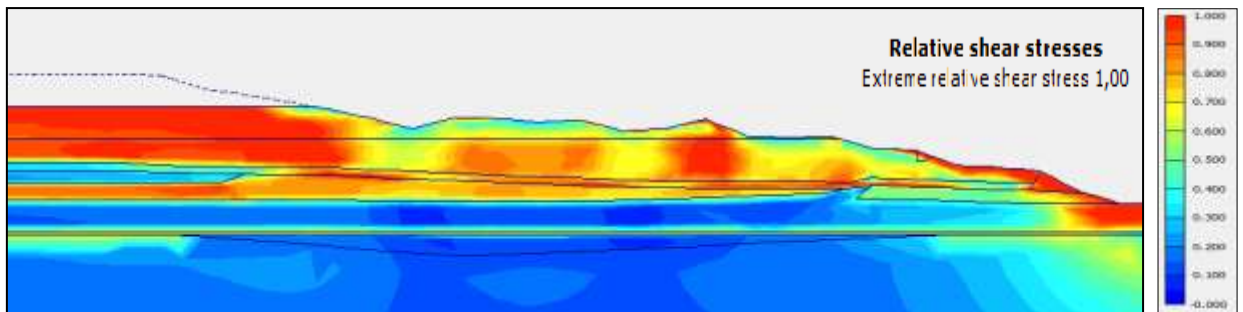
Figure 7.2.1: Relative Shear stresses after the second deposition - Study case 2 & Scenario 2.
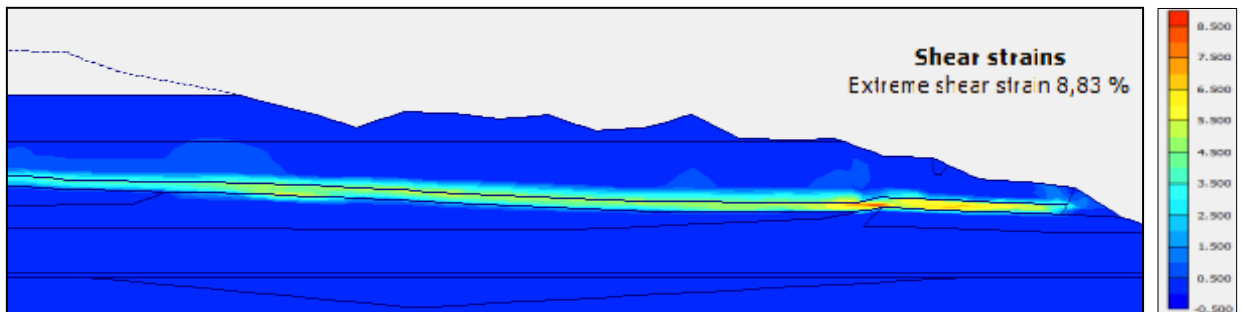
Figure 7.2.2: Shear strains after the second deposition - Study case 2 & Scenario 2.
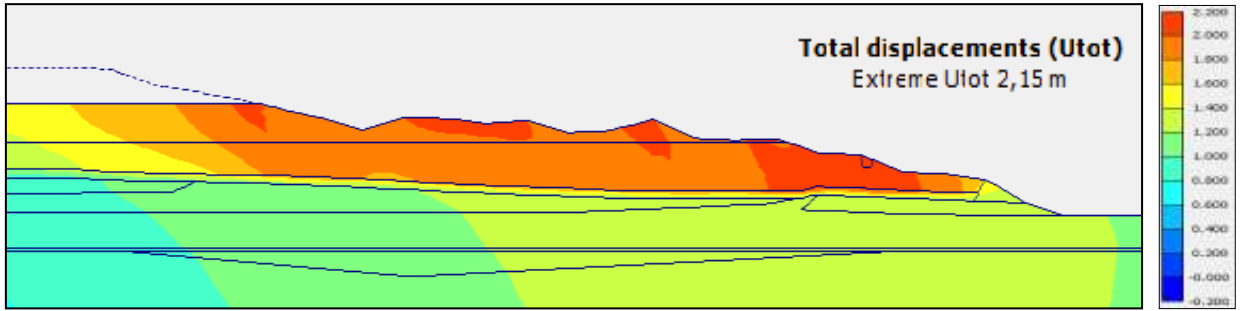
Figure 7.2.3: Maximum displacement (Utotal) after the second deposition - Study case 2 & Scenario 2.
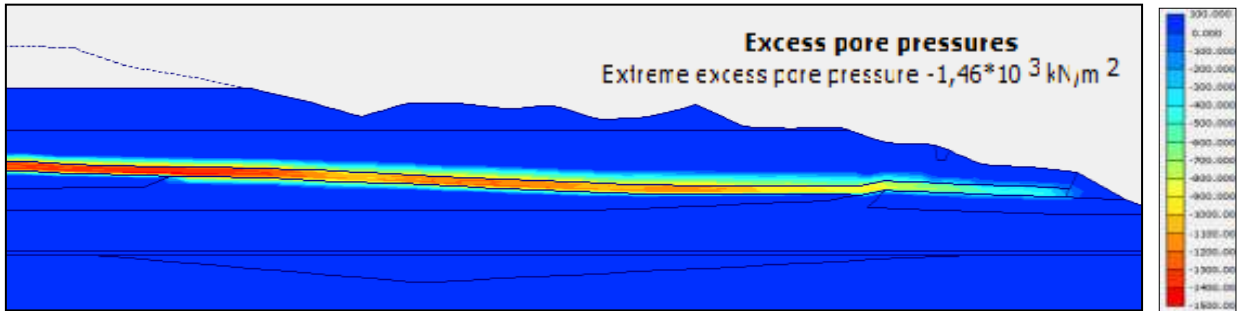

Figure 7.2.4: Excess of pore pressure after the second deposition – Study case 2 & Scenario 2.

3rd PHASE OF DEPOSITION

At the third and last deposition a 40m height of soil mass generated from mine activity was piled into the existent soil dump. Such layer was taken into considered to be drained.
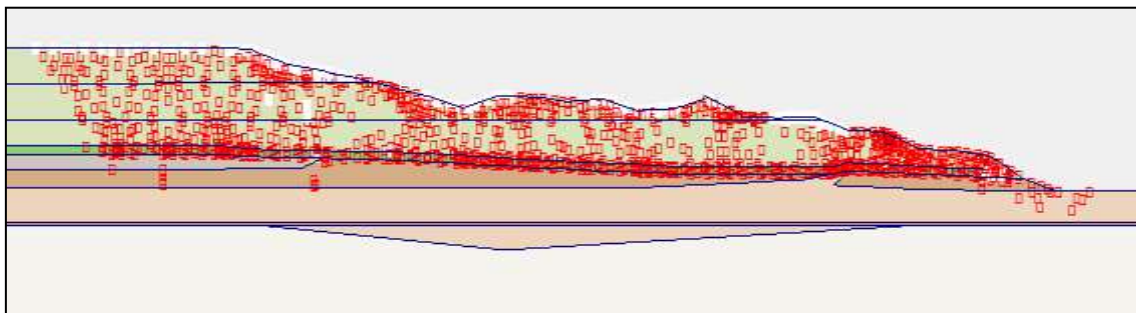
Figure 7.3: Distribution of the plastic points after the third deposition - Study case 2 & Scenario 2.
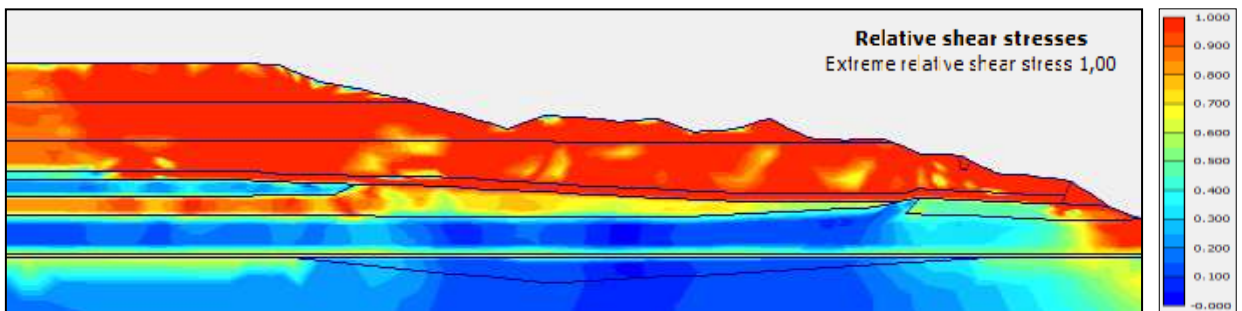

Figure 7.3.1: Relative Shear stresses after the third deposition - Study case 2 & Scenario 2.
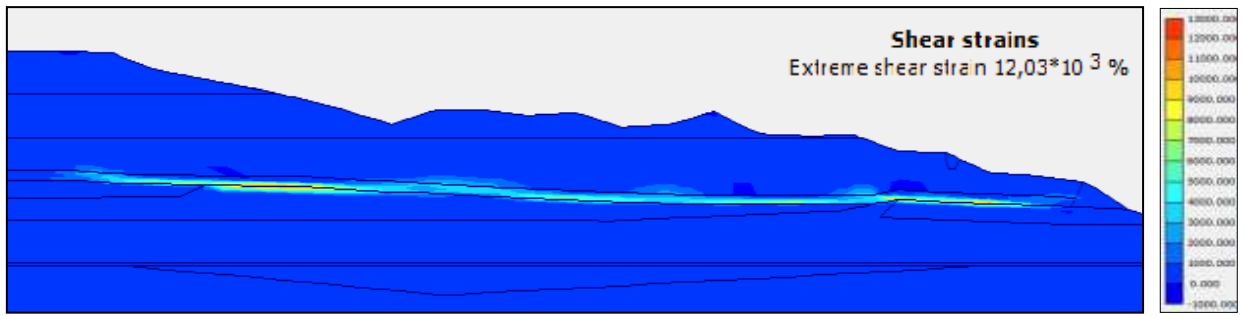
Figure 7.3.2: Shear strains after the third deposition - Study case 2 & Scenario 2.
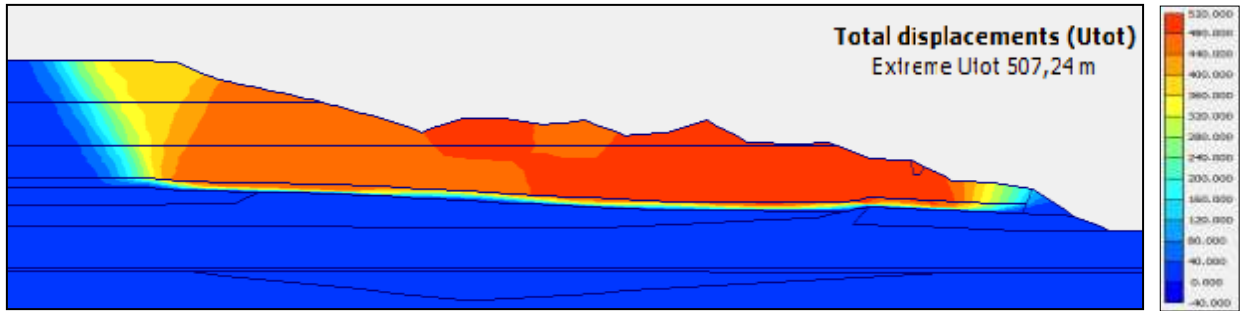

**Figure 7.3.3:** Maximum displacement (Utotal) after the third deposition - Study case 2 & Scenario 2.
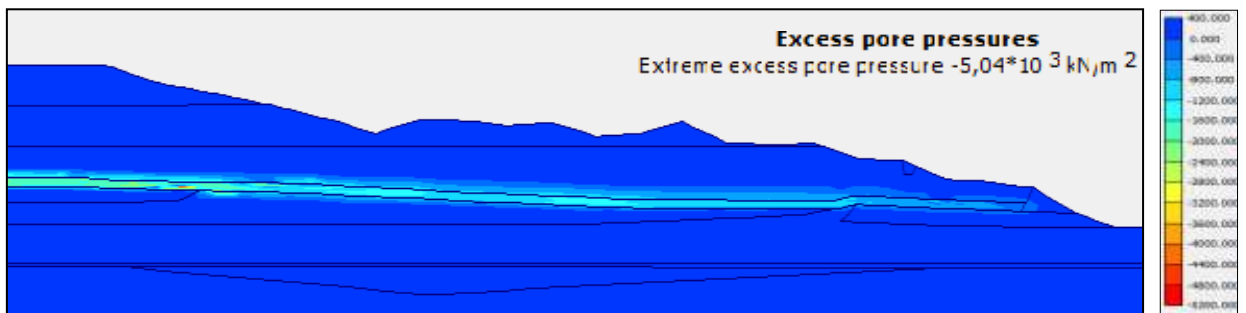
Figure 7.3.4: Excess of pore pressure after the third deposition – Study case 2 & Scenario 2.

5.6 DISCUSSION

STUDY CASE 1 | PLASTIC POINTS

- On the 1st phase of deposition when looking to the **second scenario**, we can see that is characterized by almost inexistence of plastic points in the clayey layer whereas in **first scenario**, some points are perceptible. In respect to the added layer, we can see on **second scenario**, that the plastic points are distributed within layer with a slight concentration above the spring as well as in **first scenario**.

- In the 2nd phase deposition on **second scenario** some plastic points are noticed in the clayey layer, especially near the location of the spring as well as where the conglomerate layer meets the clayey layer. On **first scenario** it is perceptible a tremendous evolution of the plastic points in the clayey layer, where they extend into the soil matrix. In both models we began to see a bond of plastic points beginning to develop after this deposition from clayey layer to the surface.

- Throughout the 3rd phase of soil deposition, on the **second scenario** we can verify that the plastic points increased exponentially along the clayey layer and in the soil mass in general, showing a well delineated path between the stability berm and top of the slope through the clayey layer where it establishes connection to the crest of the dump (near where the layer of clay and gravel ends). In **first scenario**, it was also verified a development of plastic points on the clayey layer (in which the beginning and end were similar to the **second scenario**, but with lower density of points throughout the soil matrix.

STUDY CASE 1 | RELATIVE SHEAR STRESSES

- After the 1st layer of soil added, it is verified that on **second scenario**, the clayey layer has low values of shear stresses which indicates safety is assure in this part. In the added layer we visualize some zones where the shear stresses present high values but without posing a threat to safety. At **first scenario**, the clayey layer after soil addition demonstrates significant values of shear stress, especially near the spring but without compromising safety. In relation to the added layer it is verified that in **first scenario** the values are appreciable, but not enough to put the soil matrix at risk of collapse.

- In the 2nd soil deposition it is noticed that in **second scenario**, the clayey layer shows an increment of shear stresses when compared to the first soil addition, but it is still far from presenting risks in this layer. As regards of the added layer it was verified that the shear stresses remain high, but with a reduction on shear stresses at the zone above where the conglomerate layer encounters the clayey layer. In **first scenario**, it was verified that the values of the shear stresses in the clayey layer also increased, when compared to the 1st deposition. On the soil deposit it can be seen a general increment of shear stresses on the all soil mass, with the

exception in the above area where the conglomerate layer meets the clayey layer which shows a noticeable reduction of the shear stresses.

▪ At last on the 3rd layer, it can be seen on **second scenario** that the shear stresses increase to extremely high values in the clayey layer, as well as in the rest of soil layers added presenting values around 0,9 to 1,0 where it reaches the safety limit. In the presence of this scenario, the soil eventually collapses. On **first scenario** we can see a concentration of shear stresses (red critical area) at the end of the dump model, where it extends to the stability berm by the clayey layer, in this way delineates the path where most likely the soil structure will collapse.

STUDY CASE 1 | SHEAR STRAINS

▪ Following the 1st layer of soil in the **second scenario**, with respect to the shear strains in the clayey layer, a concentration of deformations is observed after the spring location where the values are in the order of 5 %. In the added soil layer the values are almost irrelevant. On **first scenario**, the values observed in the clayey layer and on the layer of soil deposited are almost insignificant (405,76 E^{-3}).

▪ After the 2nd layer being added, the panorama remains without significant changes in the clayey layer on **second scenario**, when compared to the first deposition, being slightly larger in the order of 7 % near the stability berm. Regarding **first scenario**, the values of shear strains remain low (1,5 %), but compared with the 1st deposition start to show some regions of relevance in the clayey layer, especially after the spring location and where the conglomerate layer meets the clayey layer.

▪ Finally, in the last and third layer the **second scenario** shows a well defined line-segment within the clayey layer, where the shear strains are very high in the order of 13,80 E^3 %. In **first scenario**, is visible that the shear strains had an appreciable increment in the area where the conglomerate meets the clayey layer presenting a value of 11,78 %.

STUDY CASE 1 | MAXIMUM DISPLACEMENT (Utotal)

▪ After the 1st deposition of soil, we observed a total displacement (Utotal) of 1,34 m in **second scenario**, while in **first scenario** the Utotal was only 858,50 E^{-3} m. In both scenarios the largest displacements were surrounding the spring location.

▪ Utotal resulting from the 2nd deposition in **second scenario** was 2,0 m while in **first scenario** the Utotal was 1,38 m showing that in both cases there is a slight increase compared to the 1st soil deposition. In both scenarios, the largest displacements continue to be around the spring site.

▪ After the last layer of soil being added, there is a huge difference in results, with Utotal of 444,62 m for **second scenario** and Utotal of 2,13 m for **first scenario**. On both scenarios, the highest volume of soil moved was registered between the end line of the "clay and gravels" layer and the spring location.

STUDY CASE 1 | EXCESS PORE PRESSURE

- After the 1st deposition of the soil, it is verified in both scenarios (**first** & **second scenario**) that the clayey layer presents considerable elevated pore pressure values along its length, these being more evident near the spring site.
- In the 2nd soil deposition, it is verified in both scenarios (**first** & **second scenario**) that pore pressure keeps increasing and deviate its maximum values to the centre of the soil matrix.
- On the 3rd and last soil deposition, the same situation is verified than the previous depositions in both scenarios (**first** & **second scenario**). Where pore pressure keeps increasing, presenting values of 5,06 E^3 KN/m^2 for **second scenario**, and 1,77 E^3 KN/m^2 for **first scenario**, and diverting its maximum values to the centre of the soil mass.

STUDY CASE 2 | PLASTIC POINTS

- In the 1st phase of deposition when looking at **second scenario**, we can verify the almost non-existence of plastic points in the clayey layer, and the same applies to the **first scenario**. On the added layer, with respect to **second scenario** can be notested some points spreaded by the layer as well as some bonds starting to form from the bottom of the clayey layer to the top of deposition. On **first scenario**, the plastic points are present as well but in a small scale when compared to **second scenario**.
- With the 2nd layer of soil added, it is observed that **first scenario**, in comparison to **second scenario** shows a tremendous development of the plastic points on the clayey layer resulting in a line almost continuous, which evolves towards the interior of the soil matrix. In relation to the soil layer added in **first scenario**, there are some plastic points present, but with showing a more dispersion in **second scenario**. It should be noted that **second scenario**, the bonding of plastic points continues to develop, whereas in **first scenario**, the bonding of plastic points begins to form, starting from the bottom of the clay layer to the top of the layer of added soil, indicating where a possible soil mass rupture may occur.
- In the 3rd and last soil layer there is a overall increase of plastic points throughout the soil mass in **second scenario**, where a line of plastic points is established completely in the clayey layer, having its beginning at the edge of stability berm and binding to the top of the soil mass near where the clay and gravels layer ends. Its clear this is the path where the soil mass will collapse. The **first scenario**, also shows after the third deposition a very well defined line of plastic points in the clayey layer, which bond to the top of the soil mass in the same place of **second scenario**, being the main difference that in **second scenario**, the number and dispersion of points is higher when compared with **first scenario**, on the all soil matrix.

STUDY CASE 2 | RELATIVE SHEAR STRESSES

- After the 1st layer of soil added, it is verified that in **second scenario**, the clayey layer presents low values of shear stresses which indicates safety is assure in this part. In the added layer we visualize some zones where the shear stresses present high values but without posing a threat to safety. On **first scenario**, the clayey layer after the soil addition demonstrates significant shear stresses records especially near the spring. Regarding the added layer it is verified that in **first scenario** the values are appreciable but not enough to put the soil matrix in jeopardy.

- In the 2nd soil deposition it is noticed that in **second scenario** the clayey layer shows an increment of shear stresses compared to the first soil addition, but it is still far from presenting a risk in this layer. As regards of the added layer it was verified that the shear stresses remain high, but with a reduction on shear stresses at the zone where the conglomerate layer encounters the clayey layer. In **first scenario**, it was verified that the values of the shear stresses in the clayey layer also increased, when compared to the 1st deposition. On the soil deposit it can be seen a general increment of shear stresses in the all soil mass, with the exception in the area where the conglomerate layer meets the clayey layer which shows a reduction of the shear stresses.

- At the 3rd and last layer, it can be seen on **second scenario**, that the shear stresses increase to extremely high values in the clayey layer, as well as in the rest of soil layers added presenting values around 0,9 to 1,0 where it reaches the safety limit. In the presence of this scenario, the soil eventually collapses. On **first scenario**, we can see a concentration of shear stresses (red critical area) at the end of the dump model, where it extends to the stability berm by the clayey layer, and where in this way delineates the path where most likely the soil structure will collapse.

STUDY CASE 2 | SHEAR STRAINS

- Following the 1st layer of soil in **second scenario**, with respect to the shear strains in the clayey layer, a concentration of deformations is observed near the stability berm where the values are in the order of 5,59 %. In the added soil layer the values are almost irrelevant. On the analysis of **first scenario** the values observed in the clayey layer are almost insignificant as well as in the layer of soil deposited.

- After the 2nd layer is added the panorama remains, without significant changes in the clayey layer on **second scenario**, in respect to the first deposition, being slightly larger in the order of 8,83 % near the stability berm. Regarding **first scenario**, the values of shear strains remain low (1,55 %), but compared with the 1st deposition start to show some regions of relevance in clayey layer especially after the spring location and where the conglomerate layer meets the clayey layer.

- Finally, in the last layer, **second scenario** shows a well defined line-segment within the clayey layer, where the shear strains are very high in the order of 12,03 E^3 %. In

first scenario is visible that the shear strains had an appreciable increment in the area where the conglomerate meets the clayey layer presenting a value of 41,01 %.

STUDY CASE 2 | MAXIMUM DISPLACEMENT (Utotal)

- After the 1st deposition of the soil, we observed a total displacement (Utotal) of 1,40 m in **second scenario**, while in the **first scenario** the Utotal was only 887,97 E^{-3} %. In both scenarios the largest displacements were surrounding the spring location.
- Utotal resulting from the 2nd deposition in **second scenario** was 2,15 m while **first scenario** the Utotal was 1,43 m showing that in both cases there is a slight increase compared to the 1st soil deposition. In both scenarios, the largest displacements continue to be around the spring site.
- After the 3rd and last layer of soil being added, there is a large difference in results, with Utotal of 507,24 m for **second scenario** and Utotal of 3,25 m for **first scenario**. In **second scenario** it is noticeable that the largest displacements occurred in the end part of the dump, while in **first scenario** occurred in the location where the waste dump start to present slope.

STUDY CASE 2 | EXCESS PORE PRESSURE

- After the 1st deposition of the soil, it is verified in both scenarios (**first** & **second scenario**) that the clayey layer presents considerable elevated pore pressure values along its length, being more clear when it become closer to the spring location.
- In the 2nd soil deposition, it is verified in both scenarios (**first** & **second scenario**) that pore pressure keeps growing but in meantime, it diverge its maximum values to the centre of the soil mass.
- In the 3rd and last soil deposition, the same situation is verified than the previous depositions in both scenarios (**first** & **second scenario**), where the pore pressure continues to increase, being 5,04 E^3 KN/m^2 for **second scenario** and 1,85 E^3 KN/m^2 for **first scenario**, and diverting its maximum values to the centre of the soil mass.

CHAPTER 06 Conclusions

Based on the results, it was deduced that the Soft Soil model enables an approximation reliable concerning the kinetic behaviour of the mass when compared with Mohr-Coulomb model approach. As an example, the total displacements simulations in both study cases, showed close values with reality.

It was also verified that the hydrogeological conditions assume an effective factor in stability, being demonstrated during the gradual deposition of the soil mass, where an increment in pore water pressure was observed along the clayey layer, due to the load that was gradually being impose by the soil mass, as well as the low permeability presented by the clayey layer. This can be observed in the geological simulations regarding the excess of pore water pressure.

This increment reveals to be the major factor of instability present on the waste dump. Therefore, all the phenomena that can affect water pressures (e.g. precipitation), must be taken into account for waste dump design. The instability caused by the increase of pore water pressure can only be treated by lowering the weight of the soil dump or considering the implementation of an effective dewatering system which will have a huge impact on the budget of the overall operations.

6.1 SUGGESTIONS FOR FUTURE RESEARCH

It would be worthwhile during upcoming projects to establish more accurate geological models and to investigate and introduce more geotechnical parameters in order to establish the most reliable soil model concerning FEM analysis.

REFERENCES

- Steiakakis E., Kavouridis K., Monopolis D., "Large Scale Failure of the External Waste Dump at the South Field Lignite Mine, Northern Greece." Engineering Geology, vol. 104, no. 3-4, 2009, pp. 269–279, doi:10.1016/j.enggeo.2008.11.008.

- Steiakakis E., and Agioutantis Z., "A Kinetic Behavior Model at a Surface Lignite Mine, Based on Geotechnical Investigation.", Elsevier, Volume 18, Issue 5, May 2010, pages 558-573.

- Steiakakis E., Thalassinakis J., Agioutantis Z., Galetakis M., "Failure process of the external waste dump of a lignite mine using Finite Element Method (FEM)" at 13th ISCSM 2016, Belgrade.

- Soil Mechanics by Craig, R.F. 6th Edition, Spon Press, 1997, pages 103-108.

- Chaulya, S. K., and G. M. Prasad. Sensing and Monitoring Technologies for Mines and Hazardous Areas Monitoring and Prediction Technologies. Elsevier, 2016. Chapter 1 - Slope Failure Mechanism and Monitoring Techniques, pages 1-86.

- Duncan, J. M. - State of the Art: Limit Equilibrium and Finite-Element Analysis of Slopes, Journal of Geotechnical and Geoenvironmental Engineering, Volume 122 - July 1996, pages 577-596.

- Orman M., Peevers R., Sample K., Waste Piles and Dumps. SME Mining Engineering Handbook, 3rd ed; Darling, P., Ed.; SME: Englewood, CO, USA, 2011; Volume 1, pages 667–680.

- British Columbia Mine Dump Committee and Piteau Engineering Ltd Investigation and design of mine dumps: interim guidelines. The Committee, Victoria, B.C, 1991, pages 77-100.

- Caldwell, J.A. and Moss, A.S.E. (1981). The Simplified Analysis of Mine Waste Embankments.

- Plaxis, (2012 a): Plaxis 2D - Reference Manual 2012. Plaxis B.V, Delft, Netherlands.

- Plaxis, (2012 b): Plaxis 2D - Material Models Manual 2012. Plaxis B.V, Delft, Netherlands.

- Plaxis 2D, 2018 – Material Models Manual, Plaxis B.V, Delft, Netherlands.

- Vermeer, P. (2002): Plaxis Bulletin No.12. June 2012. Plaxis B.V, Delft, Netherlands, Pages 2-32.

- M. Kahlström, Plaxis 2D comparison of Mohr-Coulomb and soft soil material models, Luleå University of Technology, Sweden 2013, pages 17-23.

- Robertson A.M., 1985, "Mine waste disposal: an update on geotechnical and geohydrological aspects." In: Steffen, Robertson & Kirsten, Vancouver, Canada.

- Hamdhan I. N., "Slope Stability Analysis with the Finite Element Method", Itenas Library, National Institute of Technology, Bandung, Indonesia, 2013, Pages 2 - 6.

- Dumping Waste Rock at Chuquicamata Copper Mine in Chile, by goodfreephotos.com, 2009.